AMM Program Review

Dec 17–18

Enhancing irradiation tolerance of steels via nanostructuring by innovative manufacturing techniques

Andrew Hoffman on Behalf of Haiming Wen

wenha@mst.edu

Department of Materials Science and Engineering

Department of Mining and Nuclear Engineering

Missouri University of Science and Technology

Acknowledgements

- Students and postdoc working on the project: Andrew Hoffman, Jiaqi Duan, Maalavan Arivu, Hans Pommerenke, Nathan Curtis, and Victor DeLibera.
- Rinat Islamgaliev from Ufa State Aviation Technical University is thanked for providing samples.
- Nuclear Science User Facility is acknowledged for supporting neutron irradiation work, especially Keith Jewell (NSUF Technical Lead) and Katie Anderson and Leslie Soderquist (Experiment Manager).
- Co-PIs: James Cole and Yongfeng Zhang at INL.
- This research is financially supported by U.S. Department of Energy, Office of Nuclear Energy through the NEET-NSUF (Nuclear Energy Enabling Technology - Nuclear Science User Facility) program (award number DE-NE0008524).

Why We Go into NANO

Strengthening mechanisms:

A. Work hardening: dislocation-dislocation interaction

B. Solid solution strengthening: solute-dislocation interaction

C. Particle strengthening: dislocation-particle interaction

Including precipitate strengthening and dispersion strengthening

D. Grain boundary strengthening: dislocation-grain boundary interaction

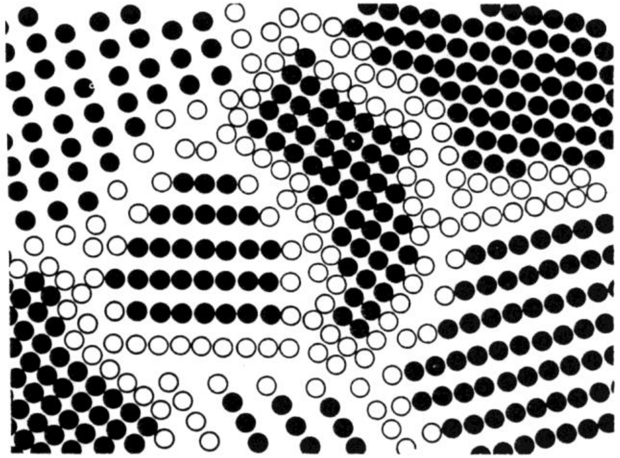

Hall-Petch relationship:

$\sigma_y = \sigma_0 + k_y \cdot d^{-1/2}$

σ_0, k_y : material constants

Nanocrystalline material: single or multiple-phase polycrystals with structural features (typically grains) smaller than 100 nm

- D=5 nm, fraction of GBs=50%
- D=100 nm~1 μm, ultrafine grained materials; D=1~10μm, fine grained materials; D>10 μm, coarse grained conventional materials

H. Gleiter, in Proceedings of the second Risϕ International Symposium on Metallurgy and Materials Science,1981, Denmark: Risϕ National Laboratory, Roskilde

GBs as Sinks for Irradiation Defects

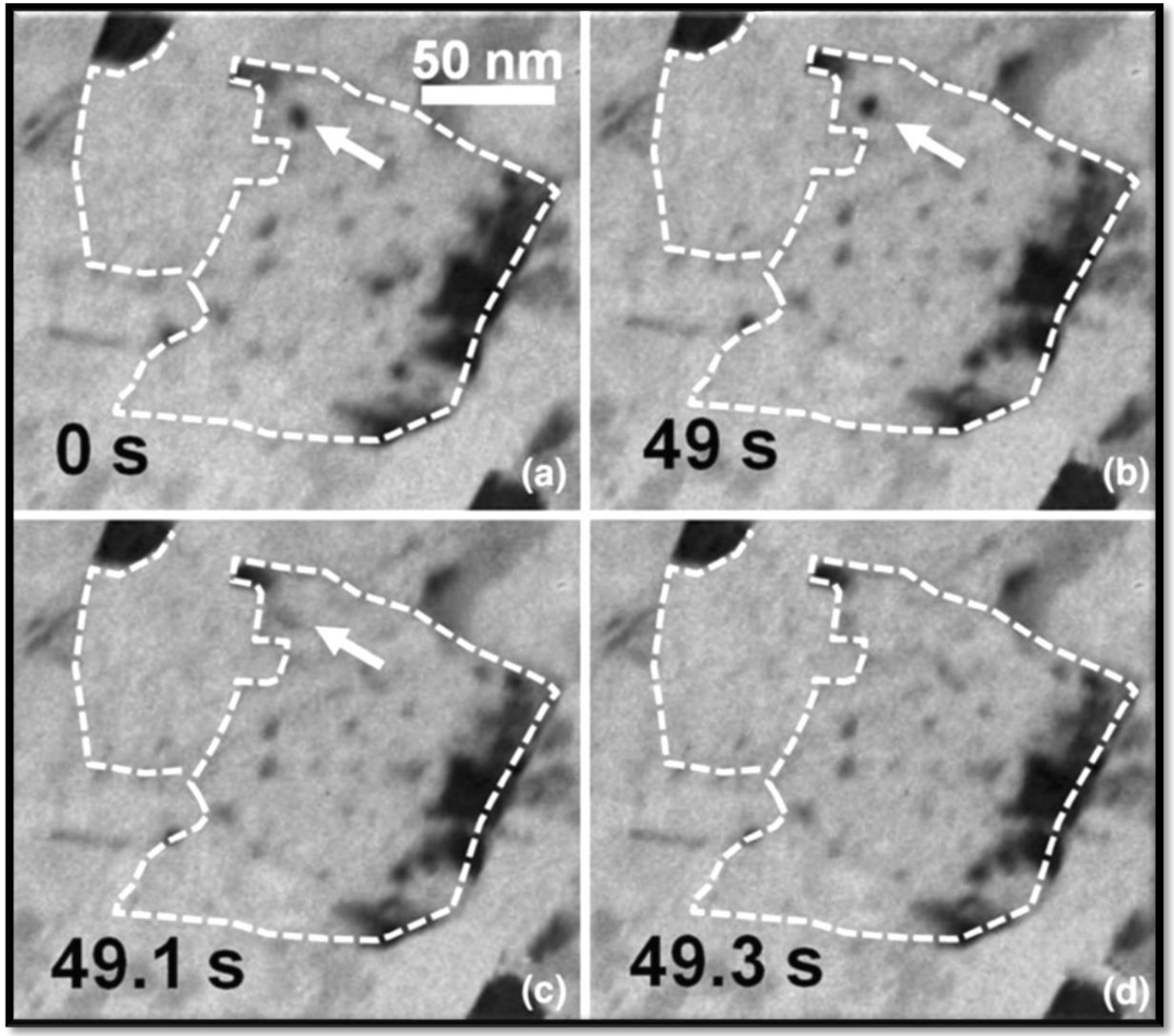

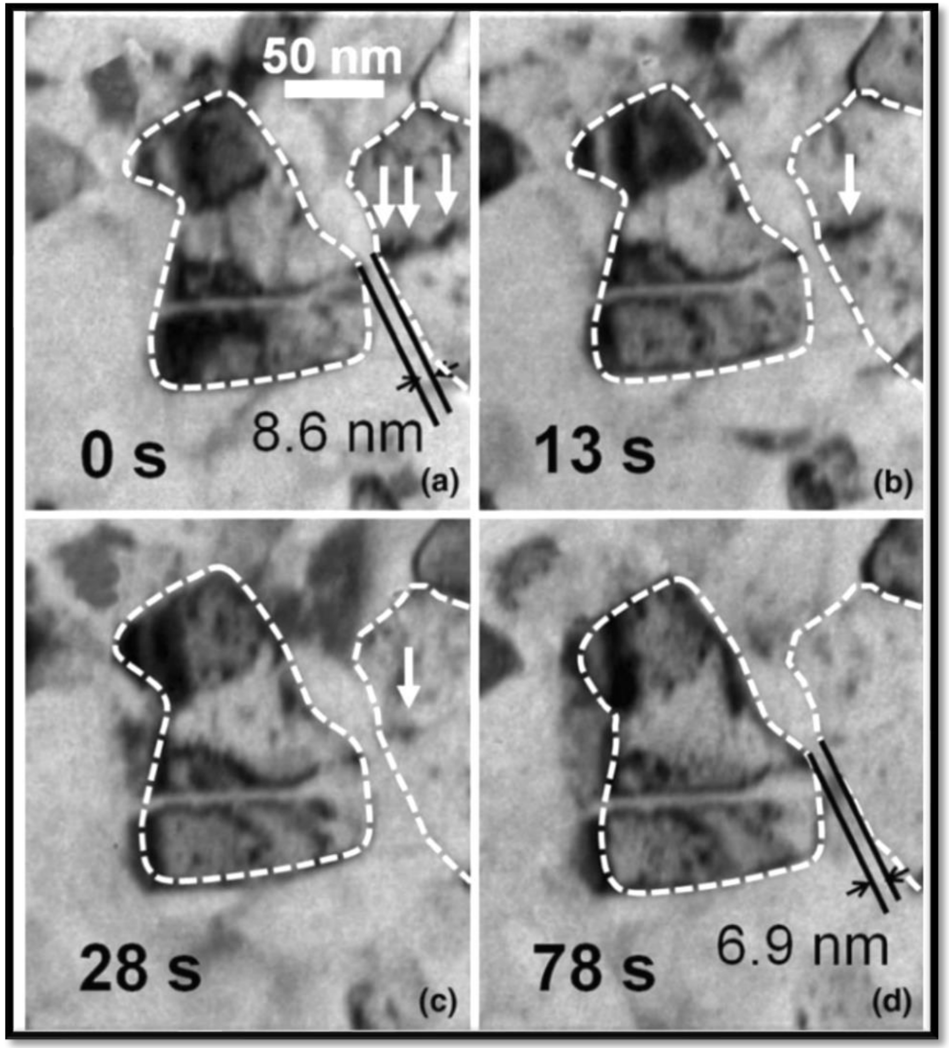

- In-situ TEM imaging during ion irradiation of NC Ni films
- Grain boundaries as sinks for irradiation-induced dislocation loops and segments

Sun C, et al., Metall Mater Trans A 44 (2013) 1966

Ion Radiation Resistance of UFG 304 Steel

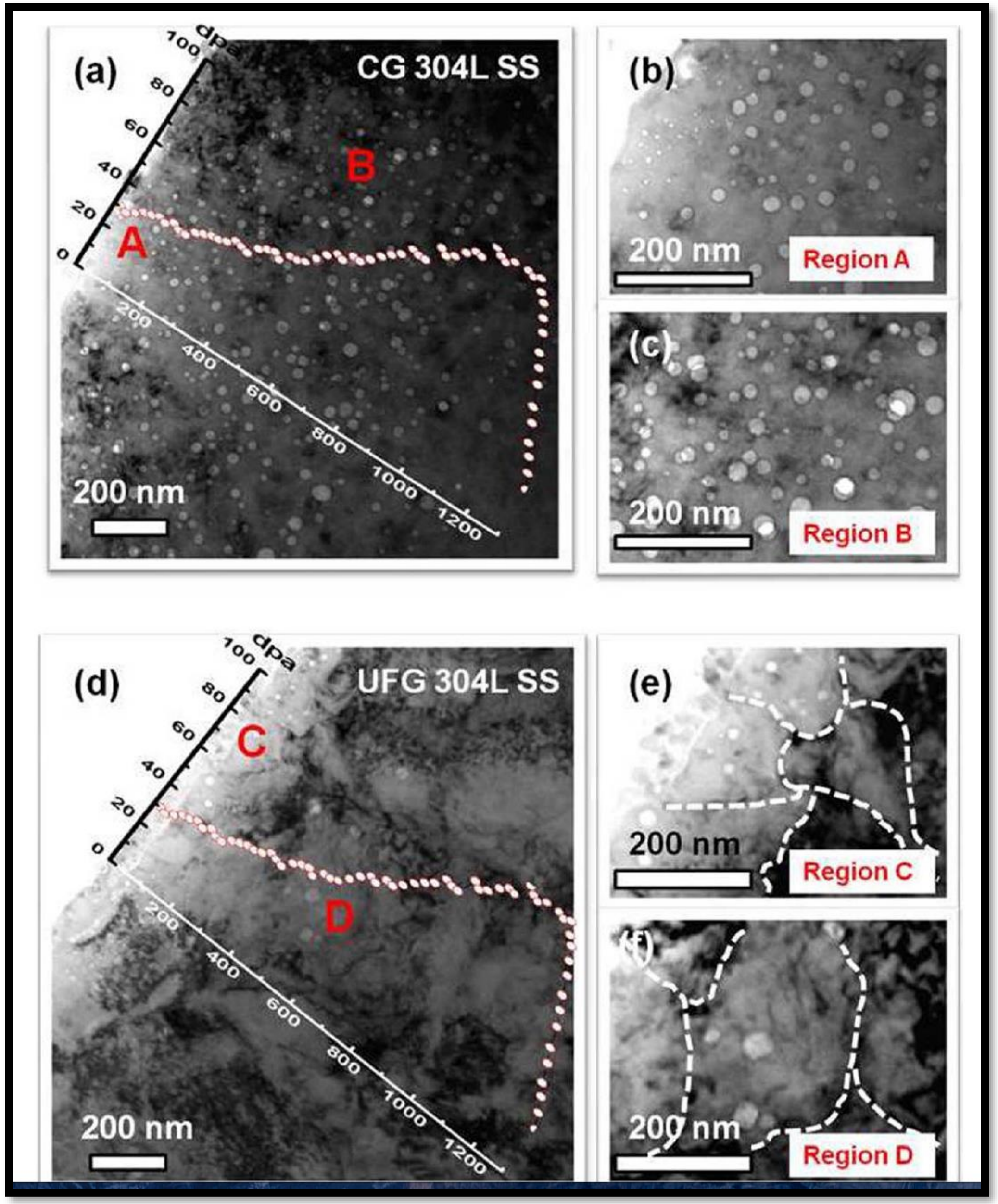

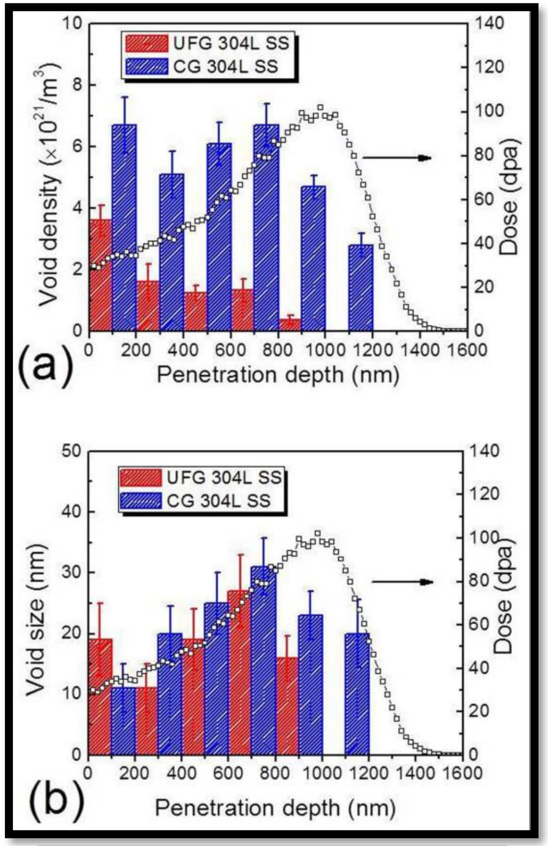

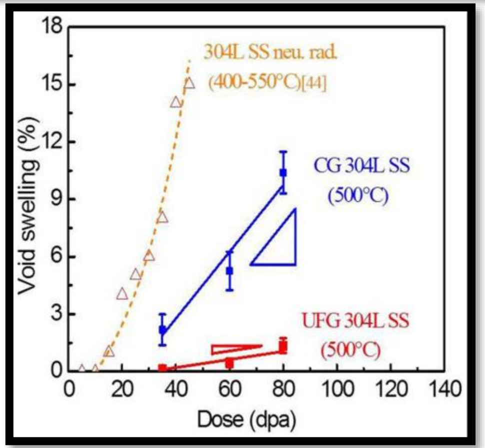

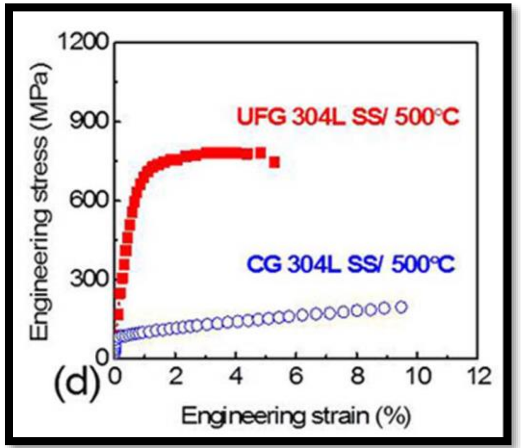

- Much smaller void density and void swelling in UFG sample
- Much higher strength of UFG sample

Sun C, et al., Scientific Reports 5 (2015) 7801

Manufacturing of bulk nanostructured metals

Grain refinement process

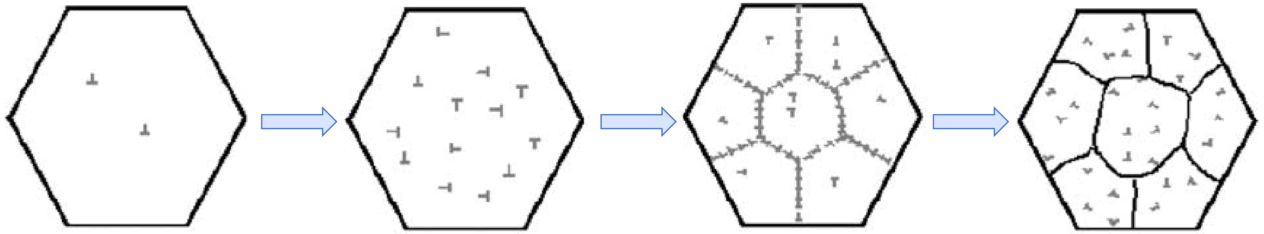

- Top-down approach
  - severe plastic deformation (SPD)
    - equal-channel angular pressing (ECAP)
    - high pressure torsion (HPT)
- Bottom-up approach
  - Step I: producing particles or agglomerates
    - inert gas condensation
    - Mechanical milling
    - chemical methods
  - Step II: consolidating particles or agglomerates
    - CIP/HIP
    - quasi-isostatic forging
    - spark plasma sintering
    - SPD
      - ECAP
      - HPT

Lavernia EJ, et al., Progress in Materials Science 51 (2006) 1

Severe plastic deformation (SPD)

High pressure torsion
(HPT)

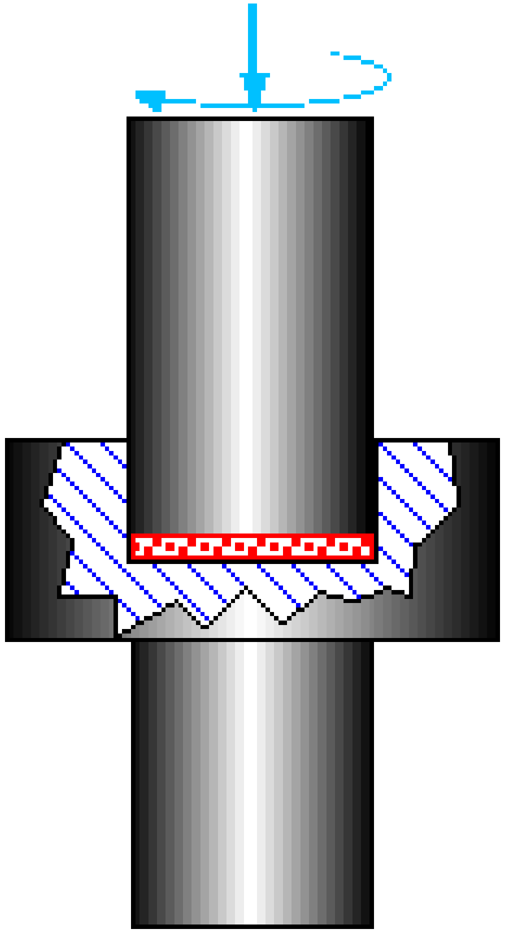

Equal-channel angular pressing
(ECAP)

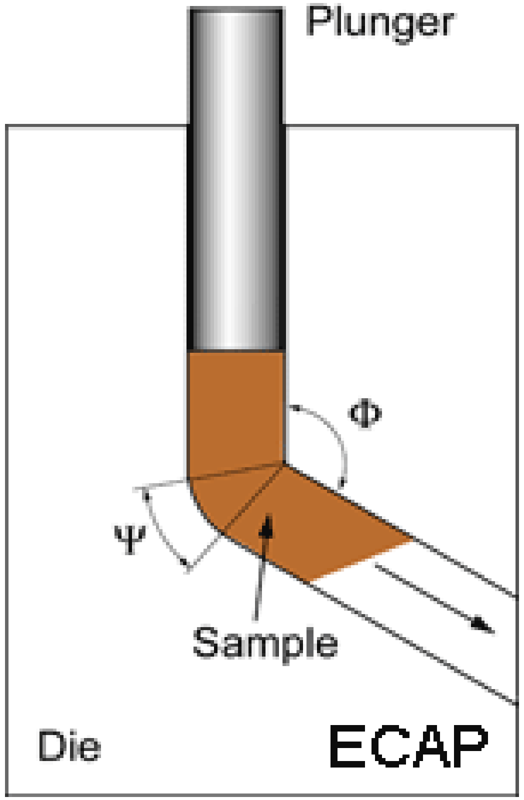

Equal-channel angular pressing

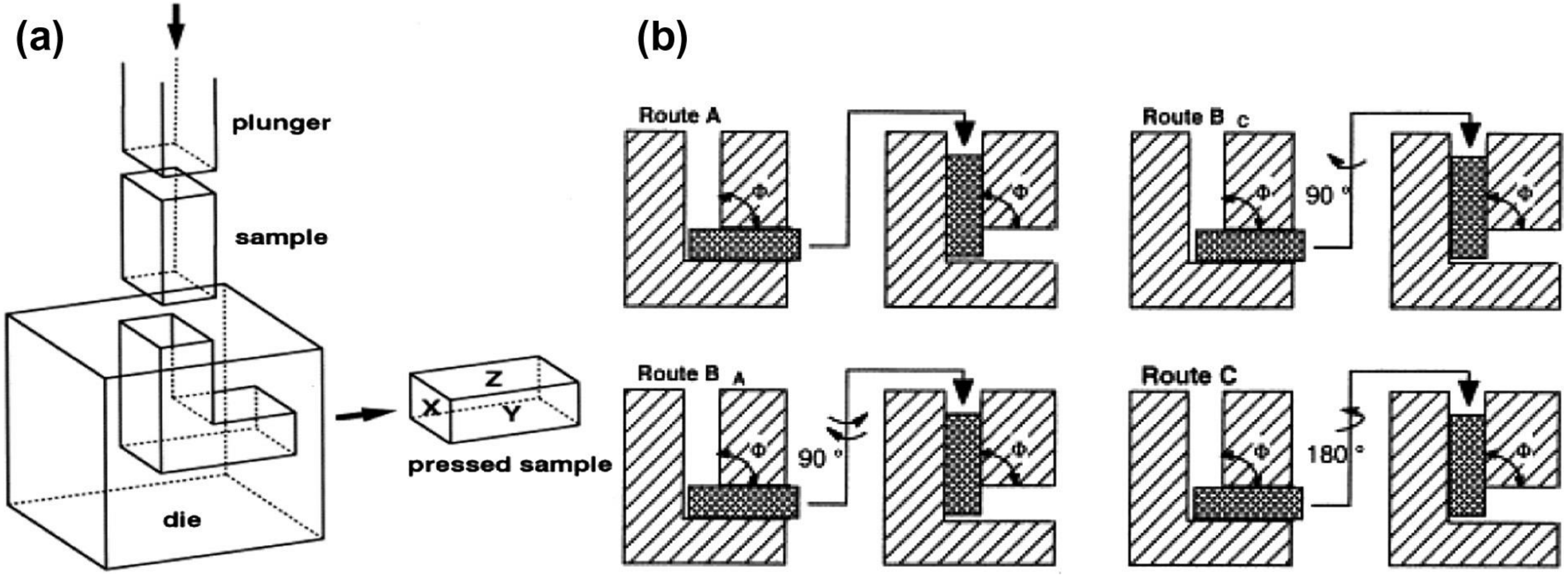

NEET-NSUF Project: Enhancing Irradiation Tolerance of Steels Via Nanostructuring

Conventionally processed (coarse-grained):
Austenitic steels
Ferritic steel
Ferritic/martensitic steel

ECAP processed (ultrafine-grained):
Austenitic steels
Ferritic steel
Ferritic/martensitic steel

HPT processed (nanocrystalline):
Austenitic steels
Ferritic steel
Ferritic/martensitic steel

Pre-irradiation examination
Mechanical testing: tension, creep
Thermal stability study: annealing
Microstructural characterization: EBSD, TKD, ASTAR, (HR)TEM, STEM, EDS, EELS, EFTEM, APT

Neutron Irradiation at ATR

Post-irradiation examination
Mechanical testing: tension, creep
Microstructural characterization: EBSD, TKD, ASTAR, (HR)TEM, STEM, EDS, EELS, EFTEM, APT

Experimental irradiation effects: irradiation-induced hardening, solute segregation, phase transformation

Modeling
Molecular dynamics,
Kinetic Monte Carlo,
Phase field

Integration and rationalization:
Differences in irradiation tolerance of ECAP, HPT and conventionally processed steels;
Mechanisms for enhanced irradiation tolerance

- Sample set 1: conventionally processed (coarse-grained) austenitic 316 steel
- Sample set 2: ECAP processed (ultrafine-grained) austenitic 316 steel
- Sample set 3: HPT processed (nanocrystalline) austenitic 316 steel
- Sample set 4: conventionally processed (coarse-grained) austenitic 304 steel
- Sample set 5: ECAP processed (ultrafine-grained) austenitic 304 steel
- Sample set 6: HPT processed (nanocrystalline) austenitic 304 steel
- Sample set 7: conventionally processed (coarse-grained) F/M Grade 91 steel
- Sample set 8: ECAP processed (ultrafine-grained) F/M Grade 91 steel
- Sample set 9: HPT processed (nanocrystalline) F/M Grade 91 steel
- Sample set 10: conventionally processed (coarse-grained) ferritic Kanthanl D
- Sample set 11: ECAP processed (ultrafine-grained) ferritic Kanthanl D
- Sample set 12: HPT processed (nanocrystalline) ferritic Kanthanl D

Funded by DOE, Office of Nuclear Energy through the NEET-NSUF program (award number DE-NE0008524). **10/1/2016 – 09/30/2023.**

Sample Preparation Using Severe Plastic Deformation

Element	SS304	SS316	G91	Kanthal-D
Fe	Balance	Balance	Balance	Balance
Cr	17.22	16.18	8.38	20.57
Ni	9.56	12.24	0.17	0.26
C	0.03	0.02	0.11	0.026
Mo	0.12	2.47	0.9	-
V	0.04	0.04	0.2	0.03
Ti	0.26	0.32	-	0.02
Cu	0.16	0.23	0.17	0.02
Si	0.24	0.37	0.46	0.24
W	0.04	0.04	-	-
P	0.03	0.03	0.01	-
Mn	-	-	0.43	0.18
Nb	-	-	0.06	-
Al	-	-	-	4.79

High pressure torsion (HPT)

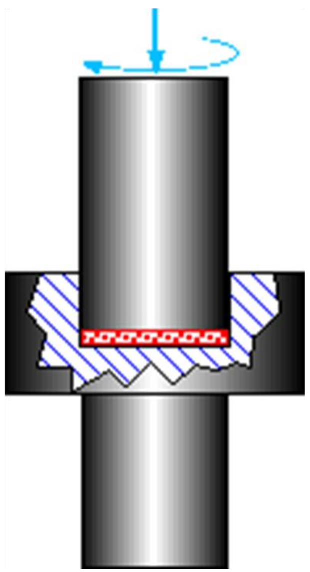

Equal-channel angular pressing (ECAP)

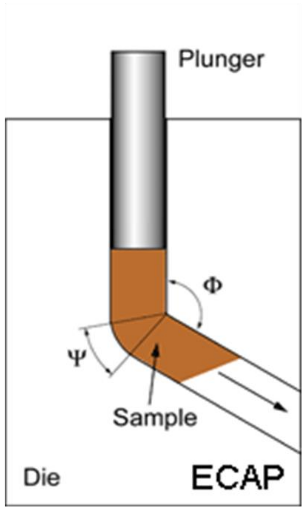

Material	Technique	Temp (°C)	# of passes/turns
SS 304	HPT	300	10
SS 316	HPT	300	10
Grade 91	HPT	300	10
Kanthal D	HPT	300	10
SS 304	ECAP	450	6
SS 316	ECAP	380	6
Grade 91	ECAP	300	6
Kanthal D	ECAP	520	6

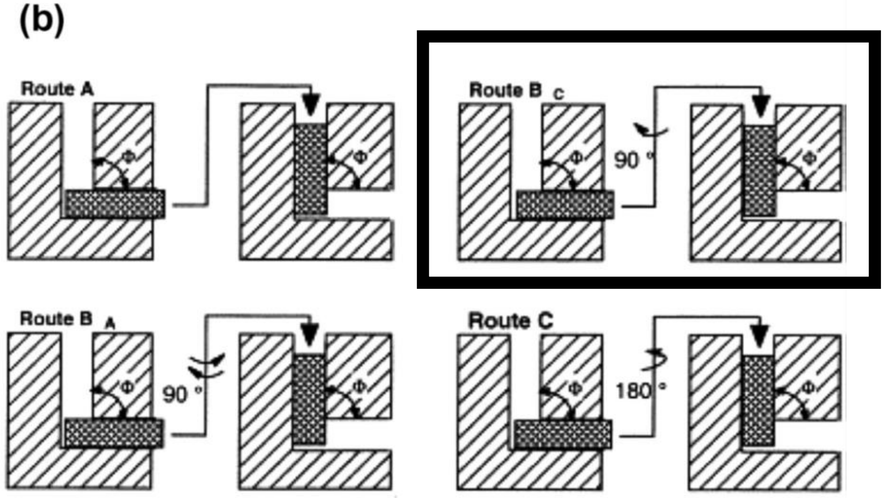

Hardness Testing of Nanostructured Steels

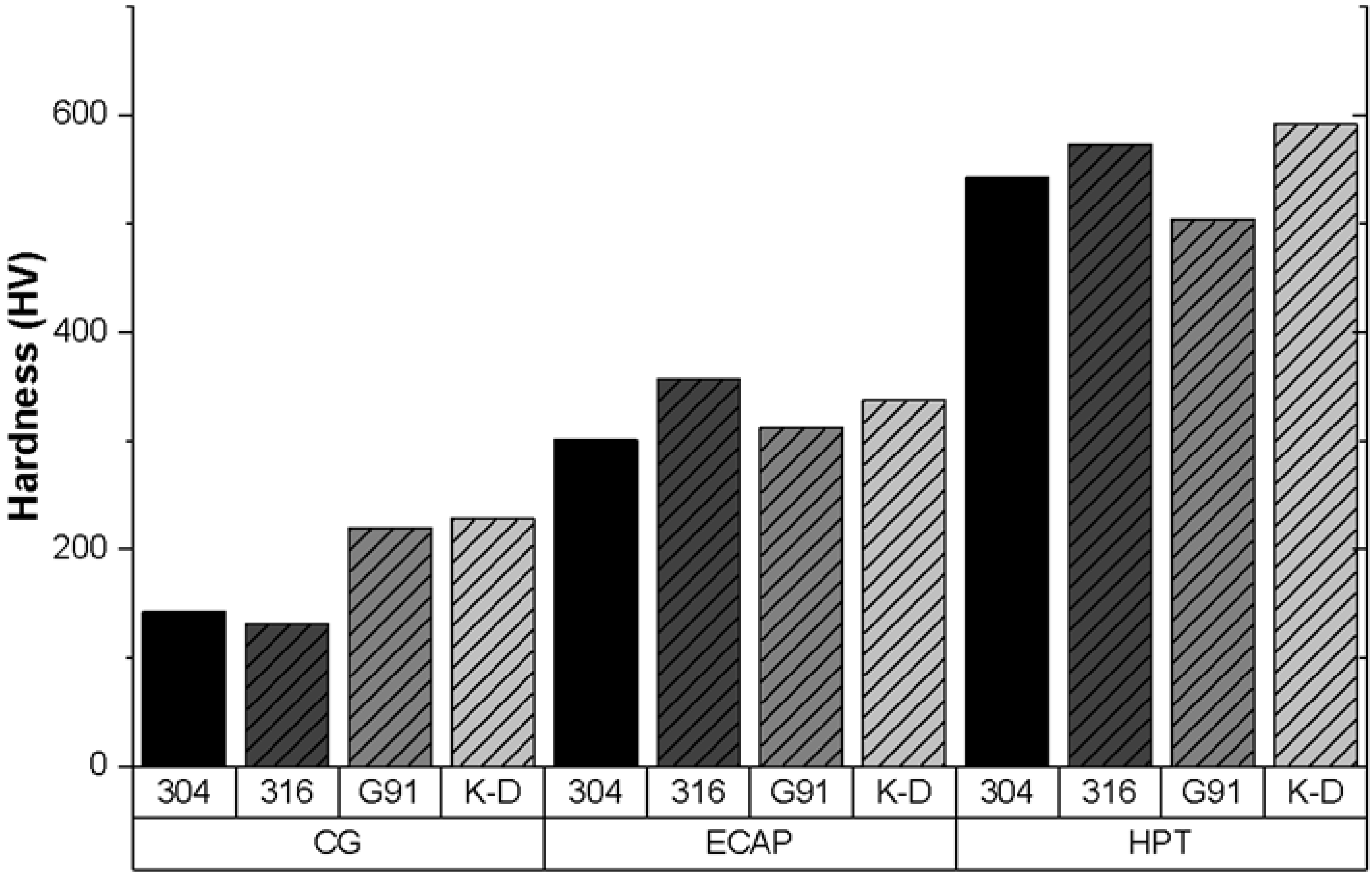

- Hardness tested using Vickers microindenter
- HPT samples having extremely high microhardness (~540 Hv)
- Hardness of HPT higher due to smaller grain size, higher strain, and more precipitate hardening
- Difference between the hardness of ECAP 316 and 304 may come from the difference in processing temperature (380 vs 450 ^oC)
- HPT samples show homogenous microstructure/grain size beyond 2mm from center of disc

Compression Testing of ECAPed Steels

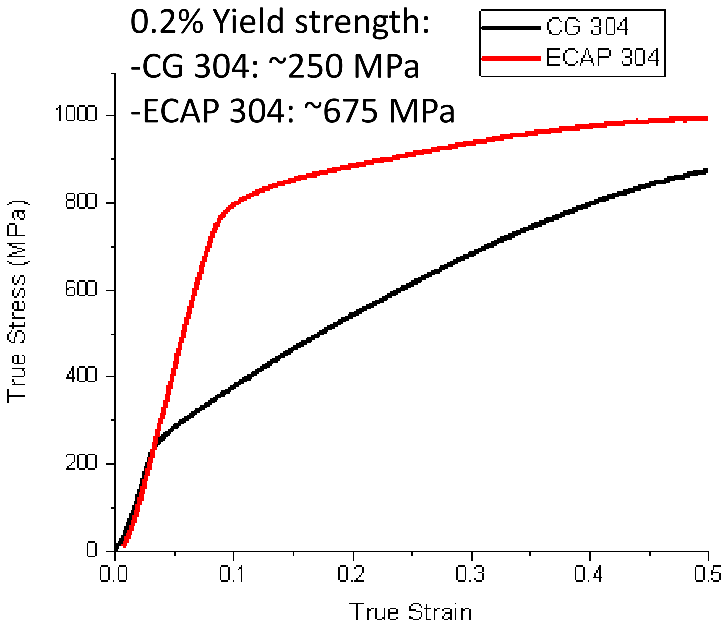

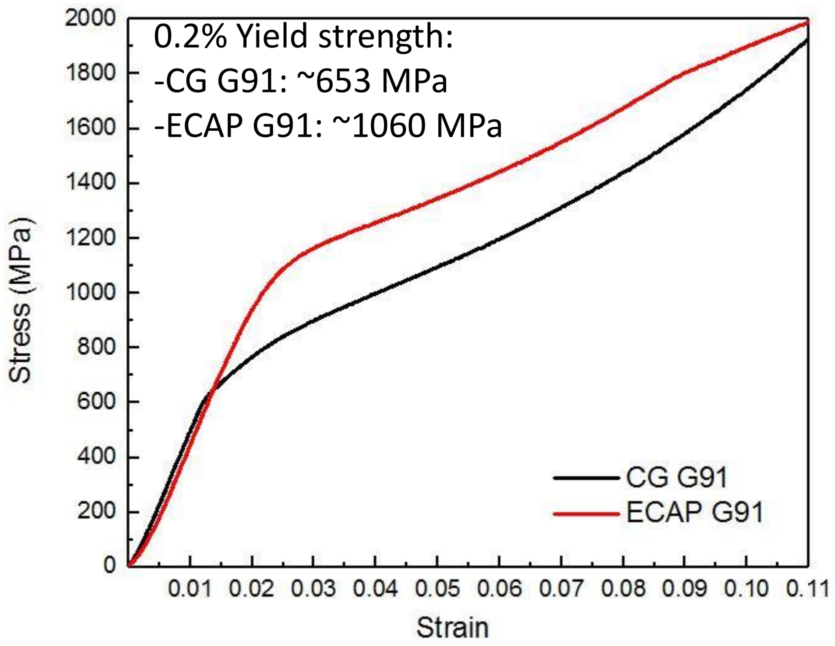

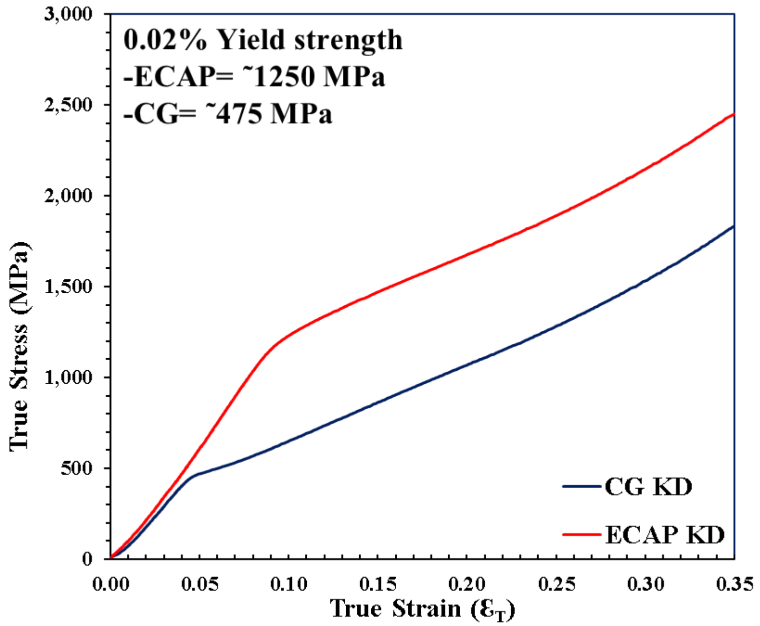

- Compression testing could not be used on HPT samples due to specimen geometry
- ECAP steels have significantly higher compressive tensile strength
- CG 304 has significantly more strain hardening than ECAP 304
  - Looking into enhanced stability of austenite phase of nanostructured steels (suppressed deformation induced martensite transformation)

SPD 304 microstructure

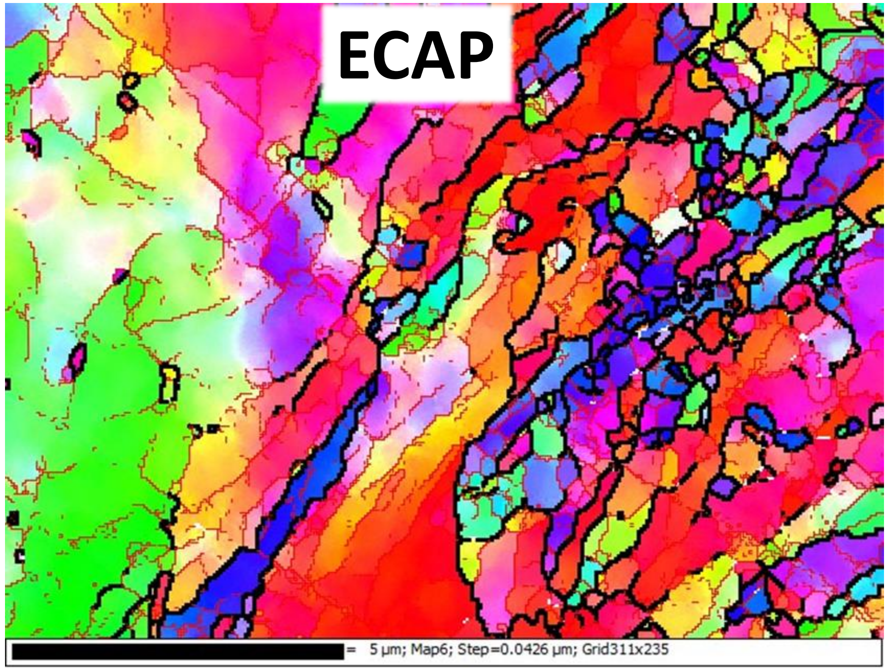

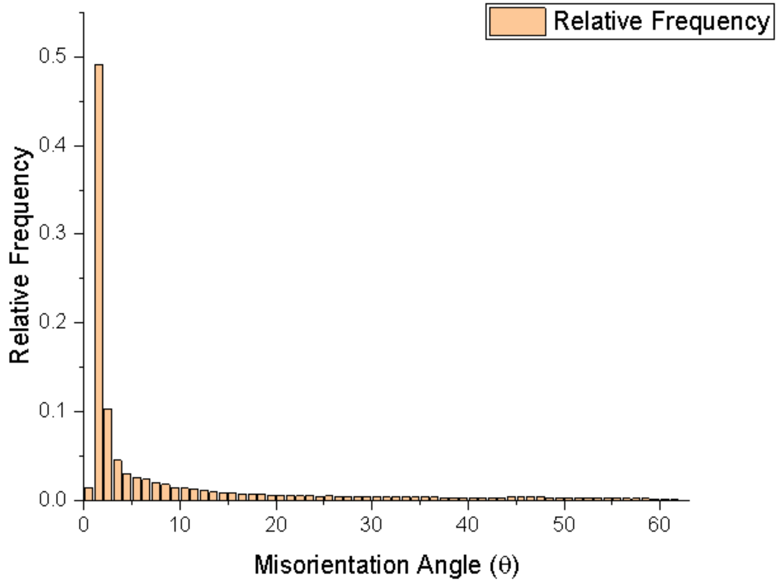

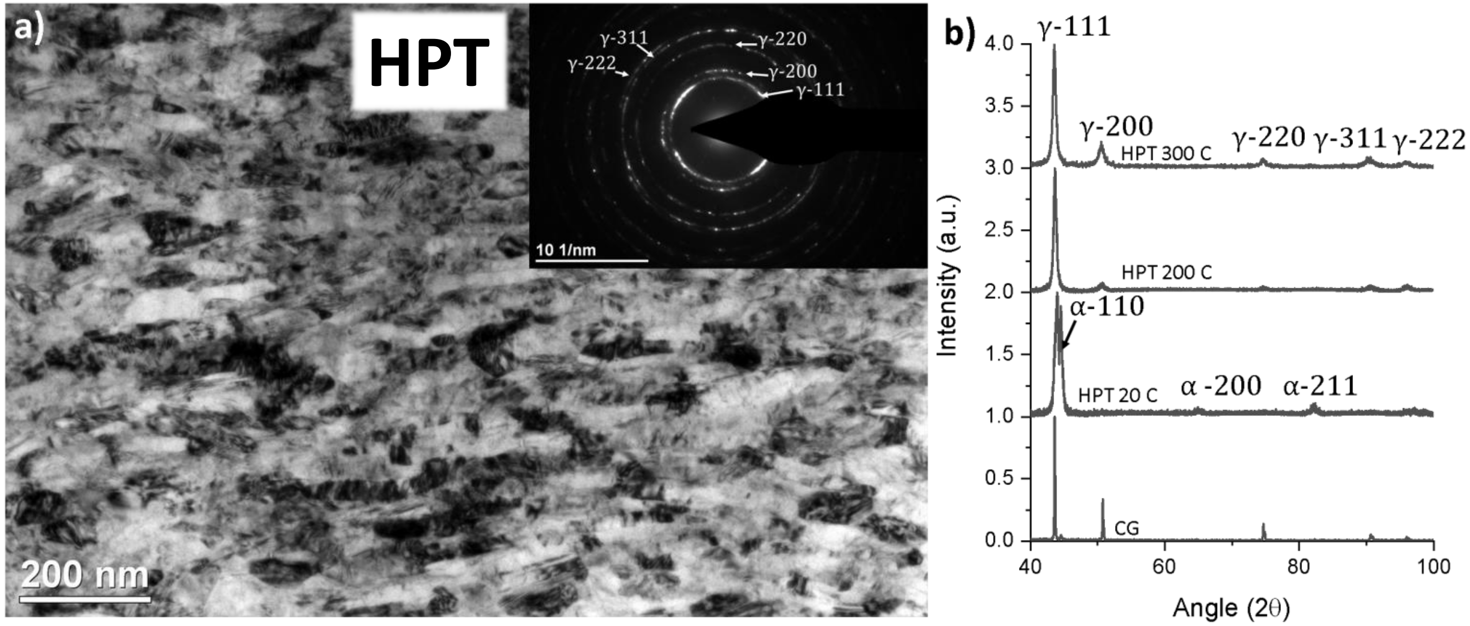

- ECAPed microstructure inhomogeneous with significant fraction of low angle grain boundaries
- HPT microstructure is homogenous with high angle grain boundaries
- Deformation at elevated temperatures important in suppressing deformation induced martensite transformation
  - All SPD austenitic samples are fully austenitic

Microstructure of ECAP G91

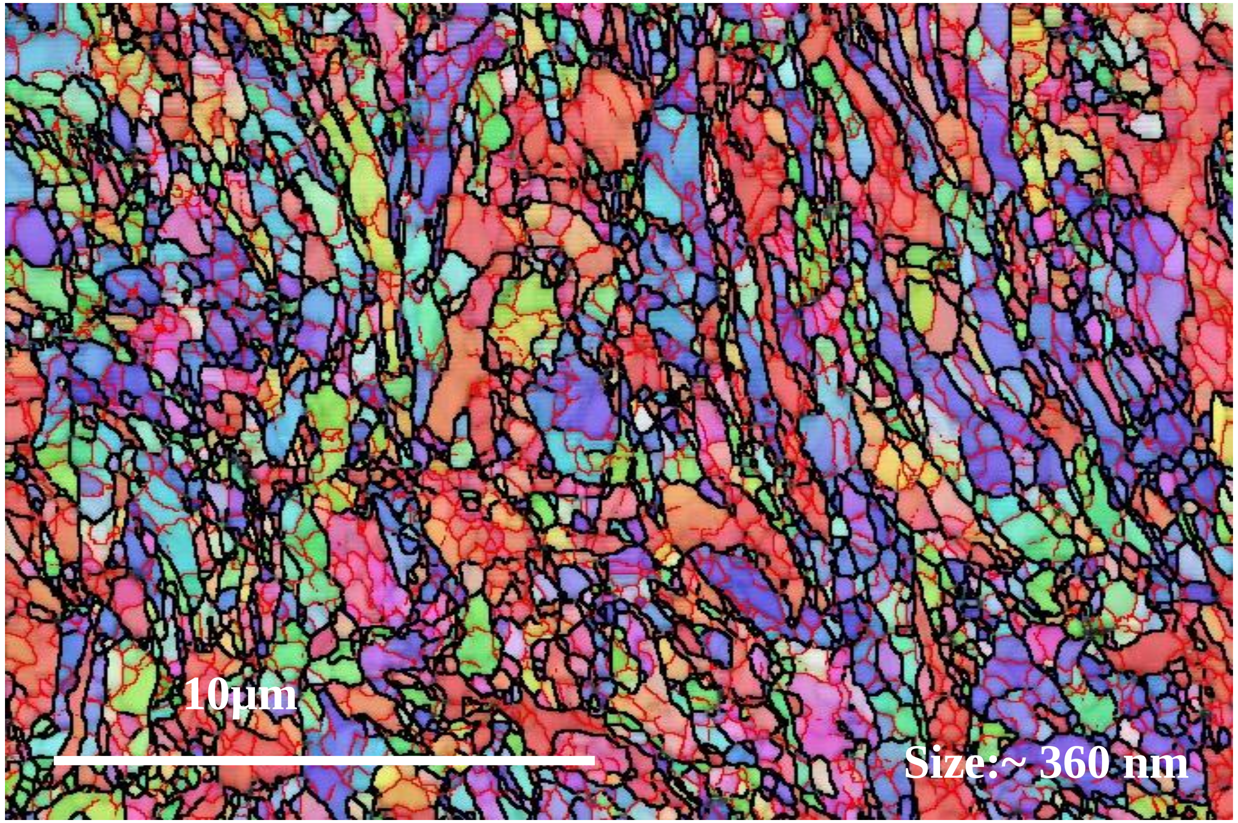

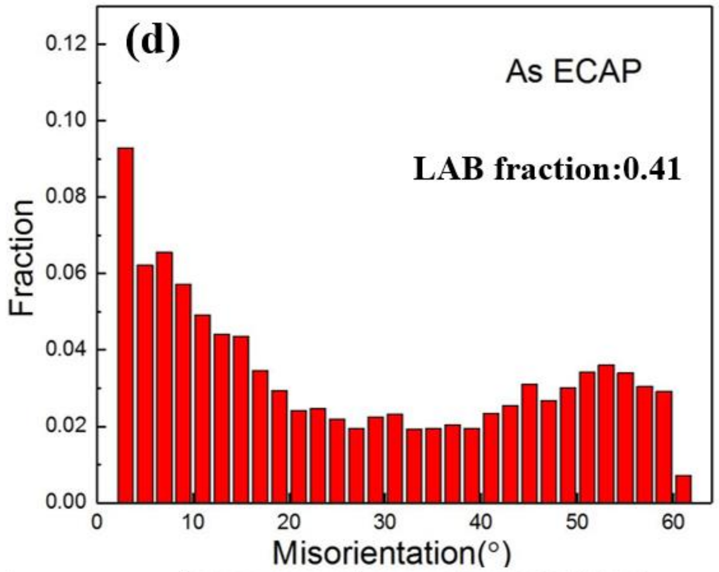

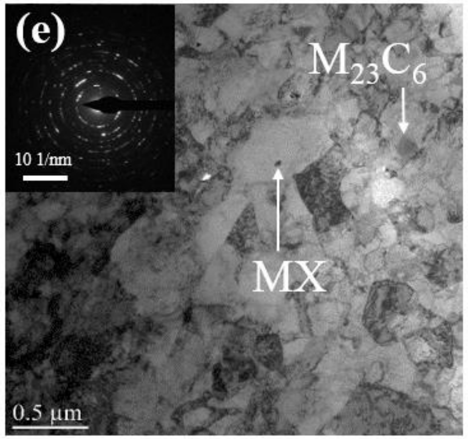

$M_{23}C_6$ M=Cr, Mo
Average: 116 nm
Number density: 0.46×10^{12} m $^{-2}$
Area Fraction: 2.1%

MX M=Nb, V
Average: 59 nm
Number density: 0.32×10^{12} m $^{-2}$
Area Fraction: 0.41%

Microstructure of HPT G91

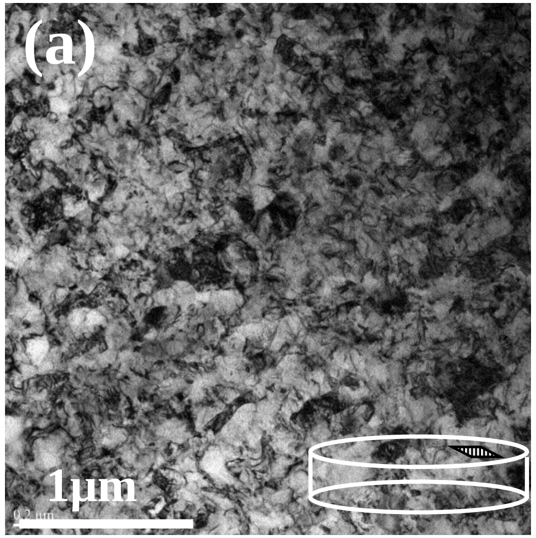

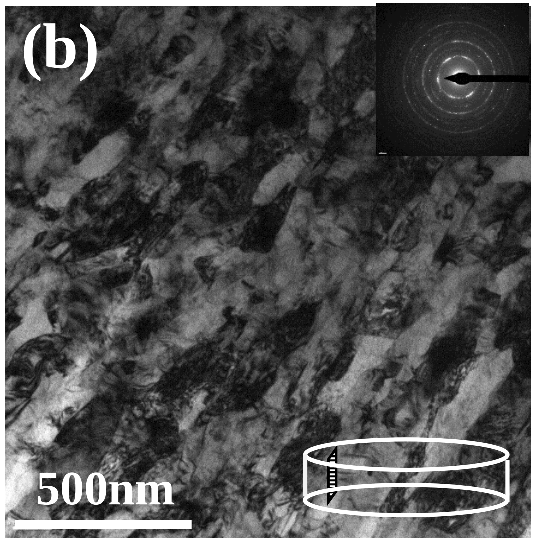

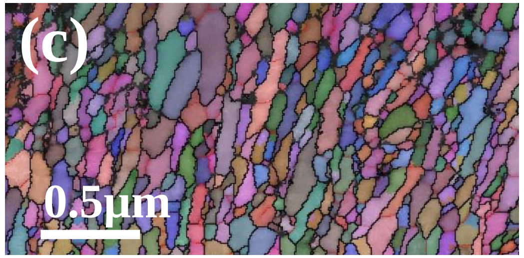

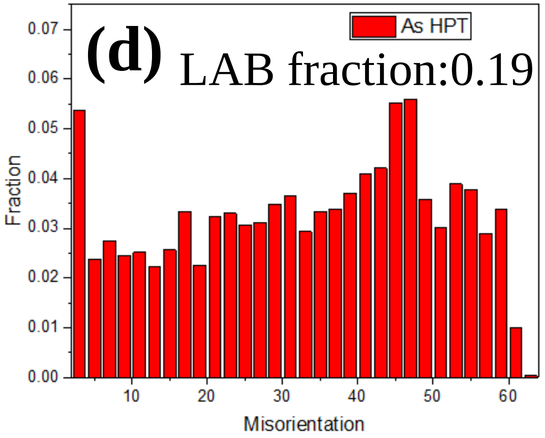

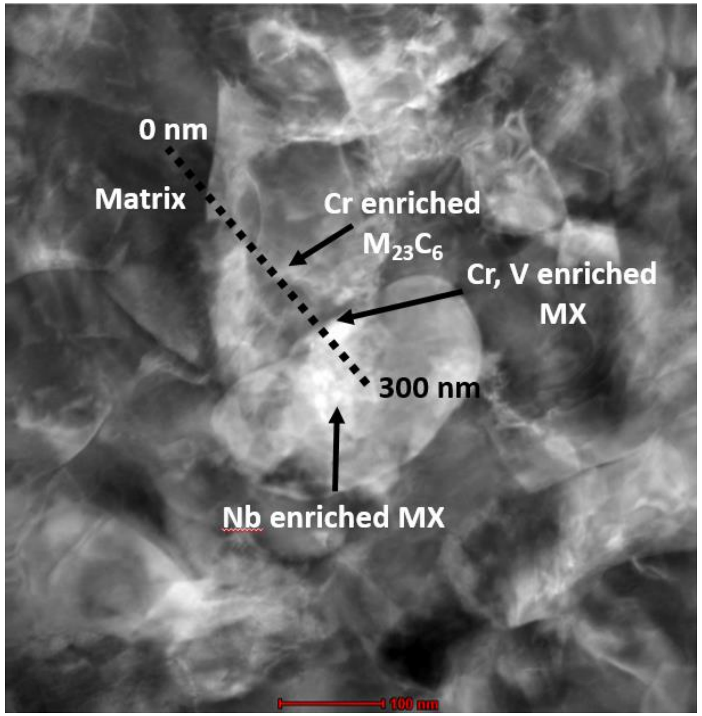

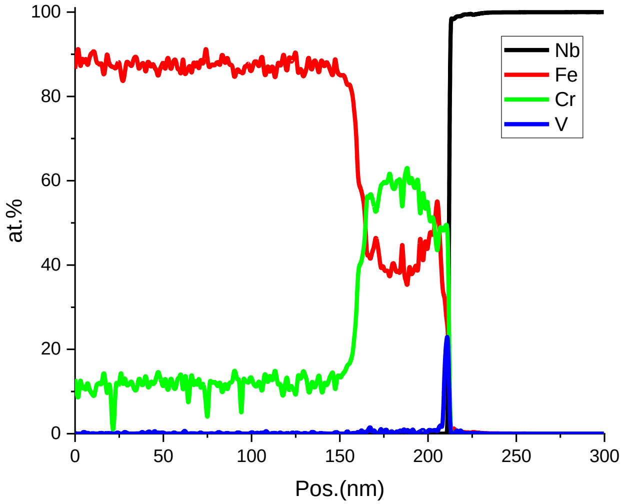

$M_{23}C_6$
Average: 47 nm
Number density: $2.7x10^{12}$ m^{-2}
Fraction: 2.3%

MX
Average: 20 nm
Number density: $3.3x10^{12}$ m^{-2}
Fraction: 0.47%

Microstructure of ECAP Kanthal-D

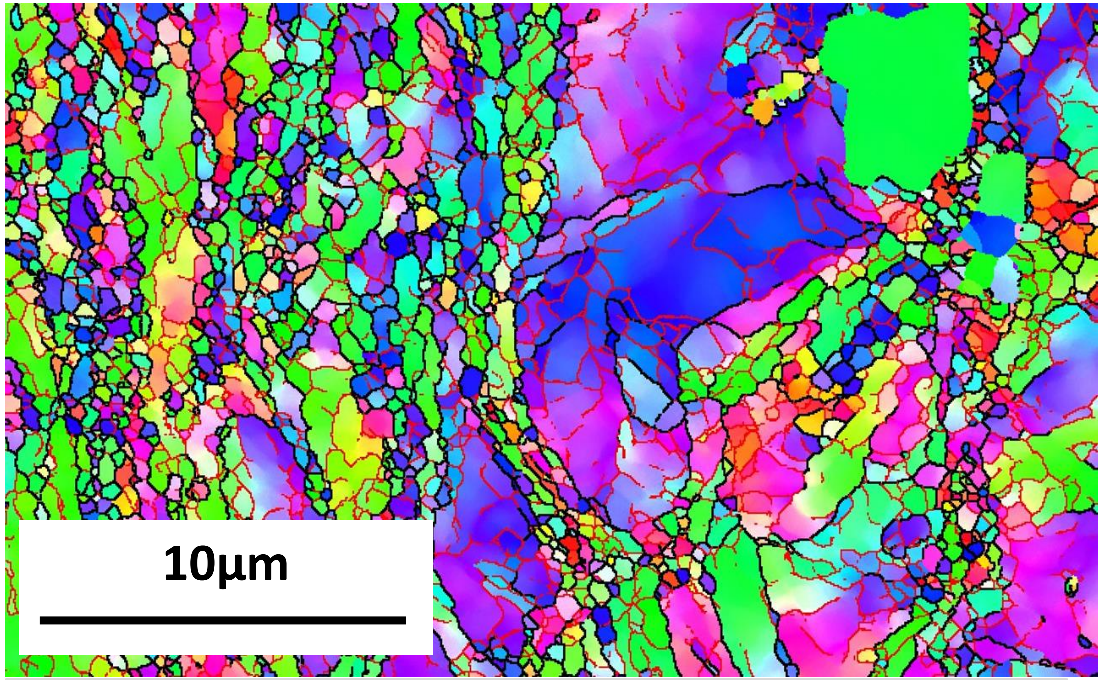

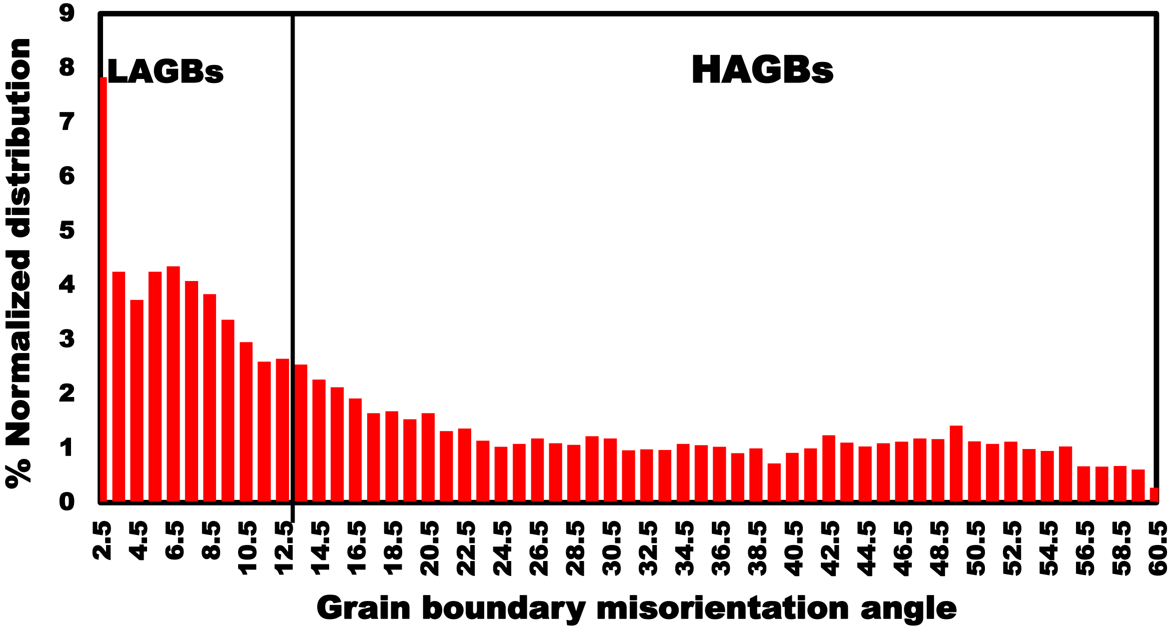

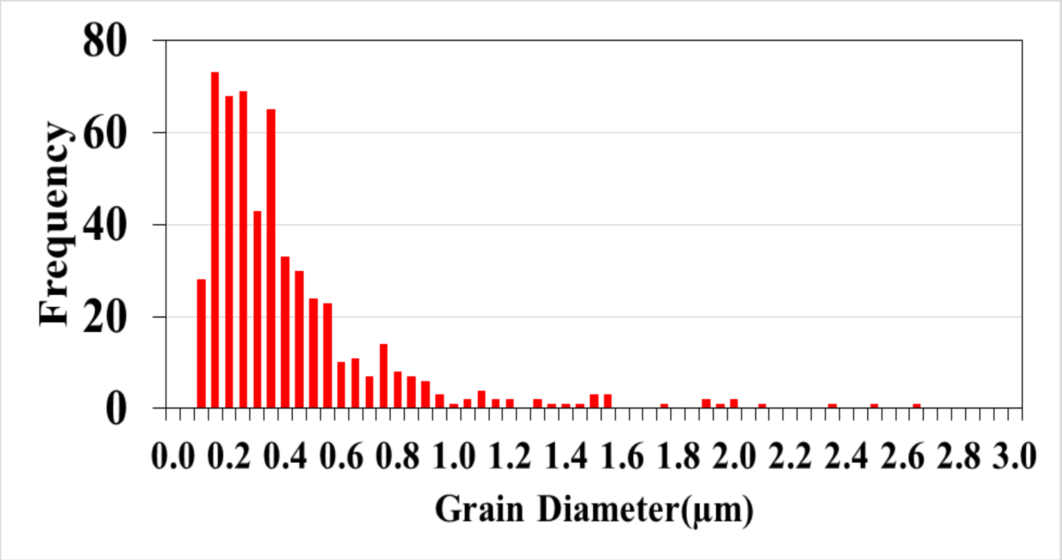

- ECAP KD has a non- homogenous microstructure.
- Multimodal grain size distribution.
- The volume fraction of low angle grain boundaries (2^o -15^o) is ˜40%.

$Cr_{23}C_6$ precipitation in ECAP and HPT FeCrAl

ECAP

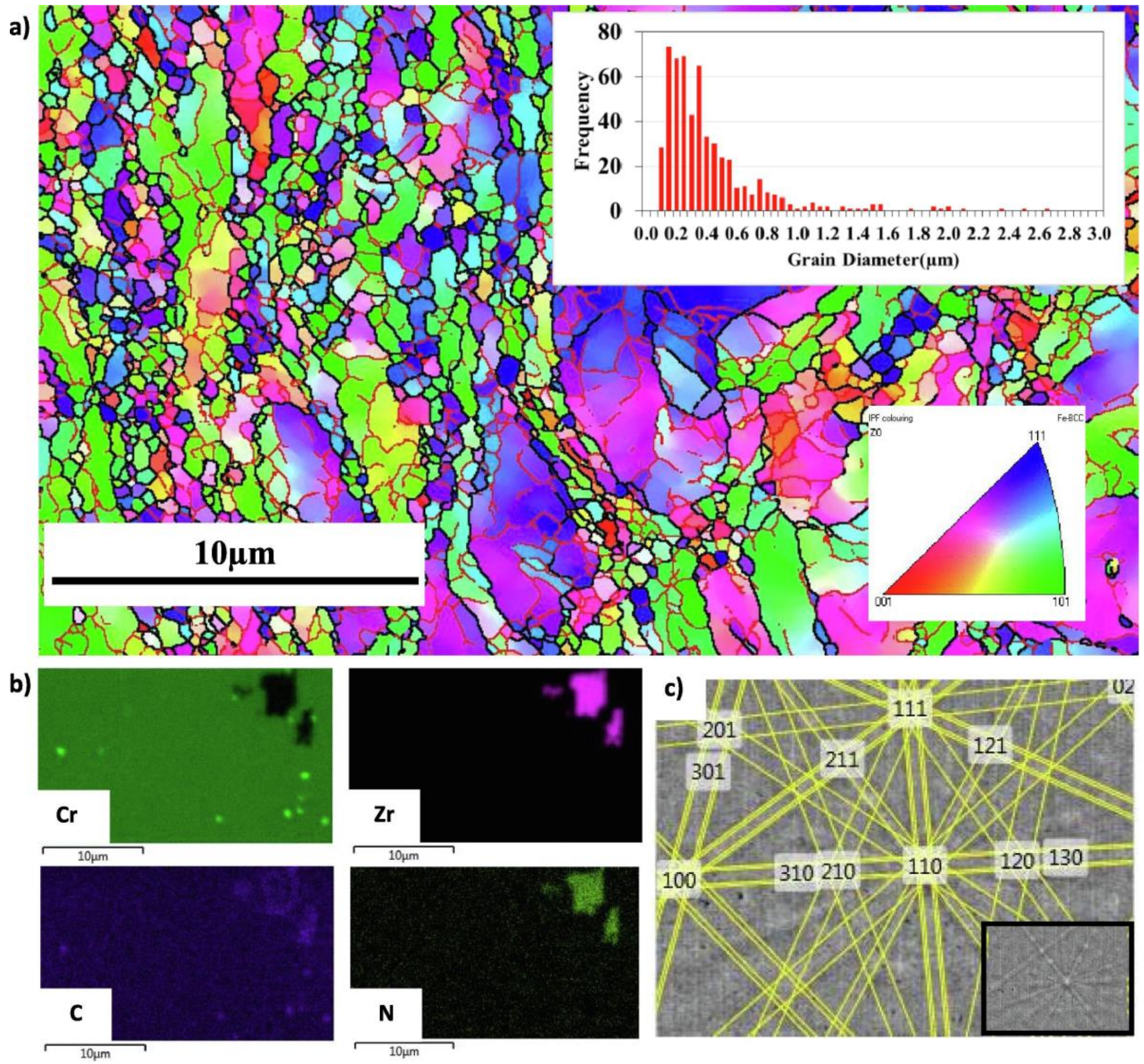

HPT

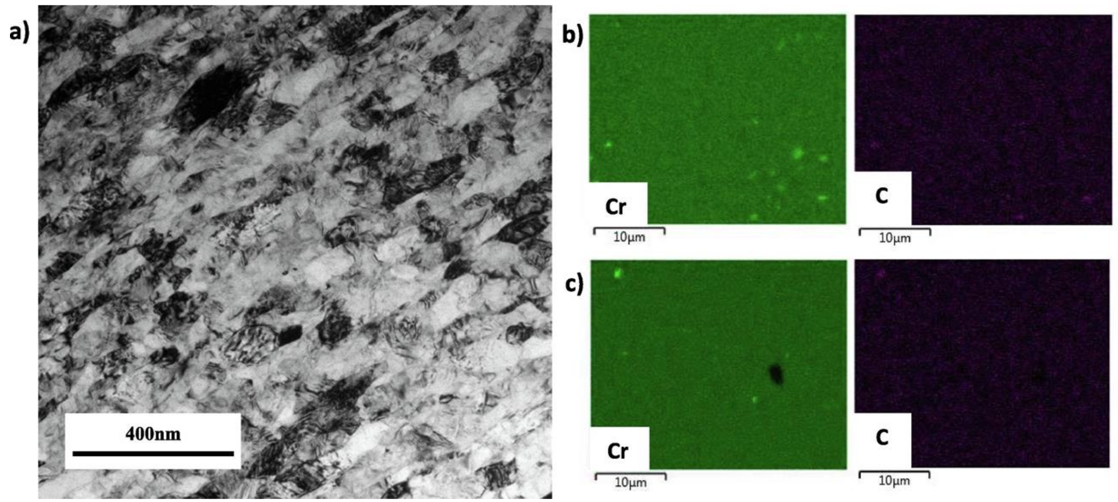

CG Annealed at 520 C

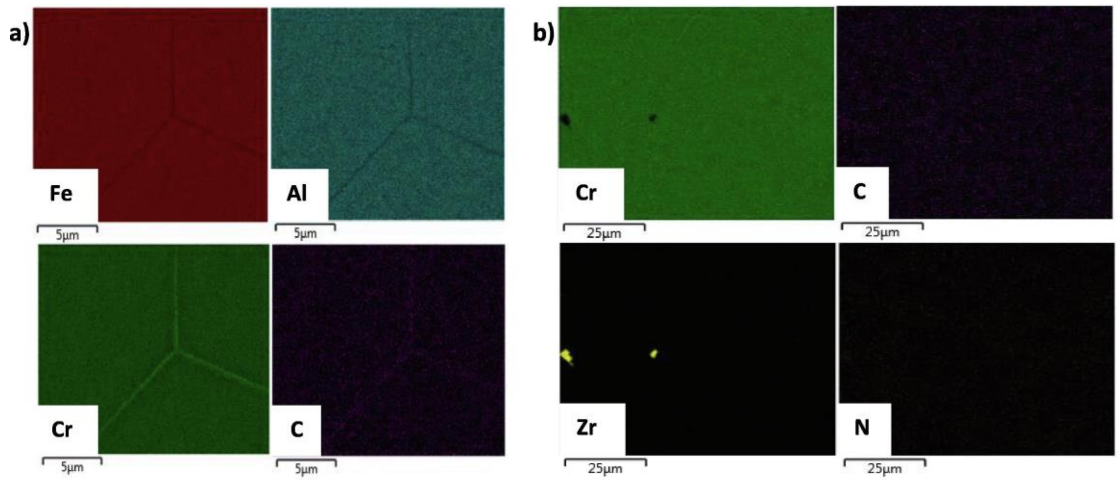

- **SPD causes Cr enriched carbide precipitation in Kanthal-D**

Segregation/Precipitation in 304 after HPT

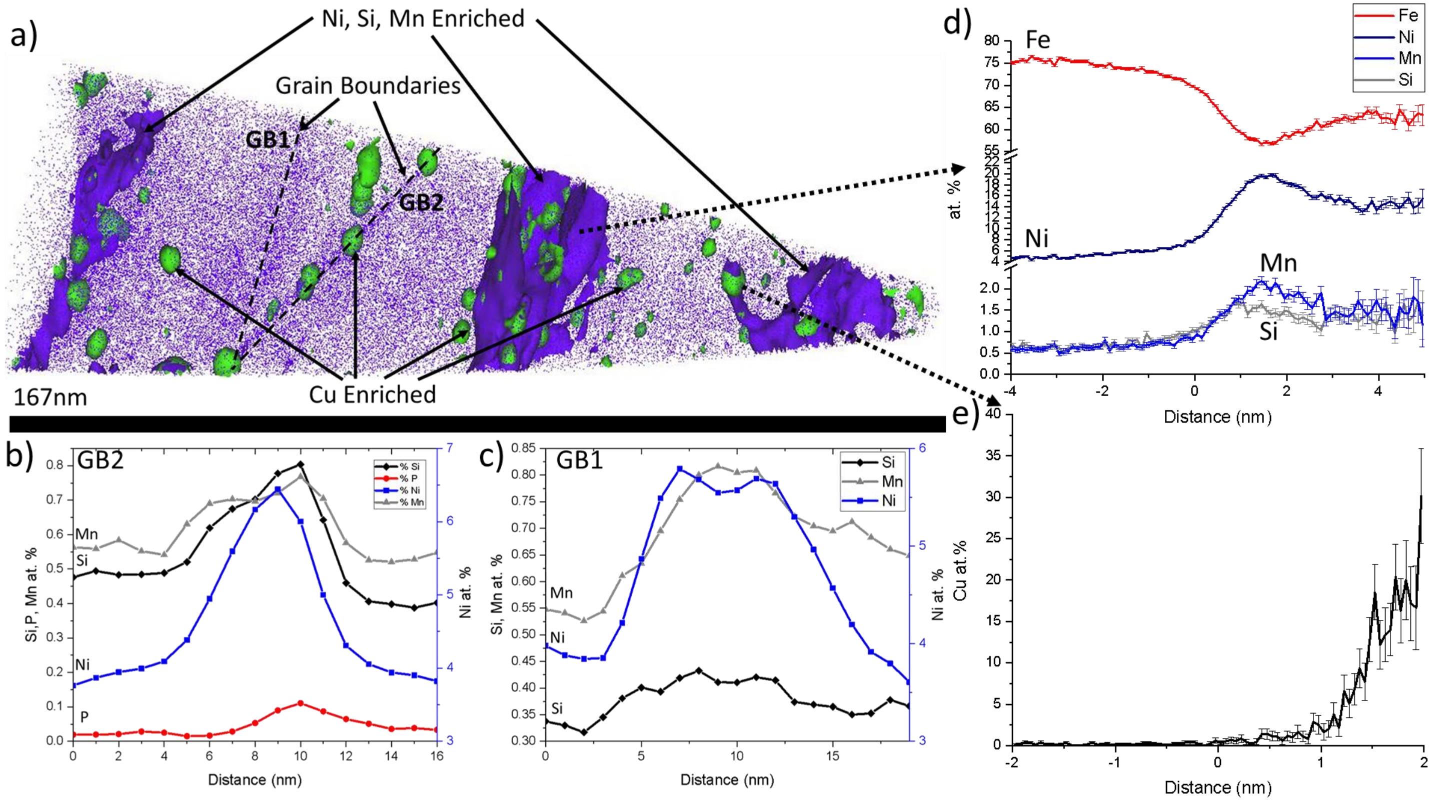

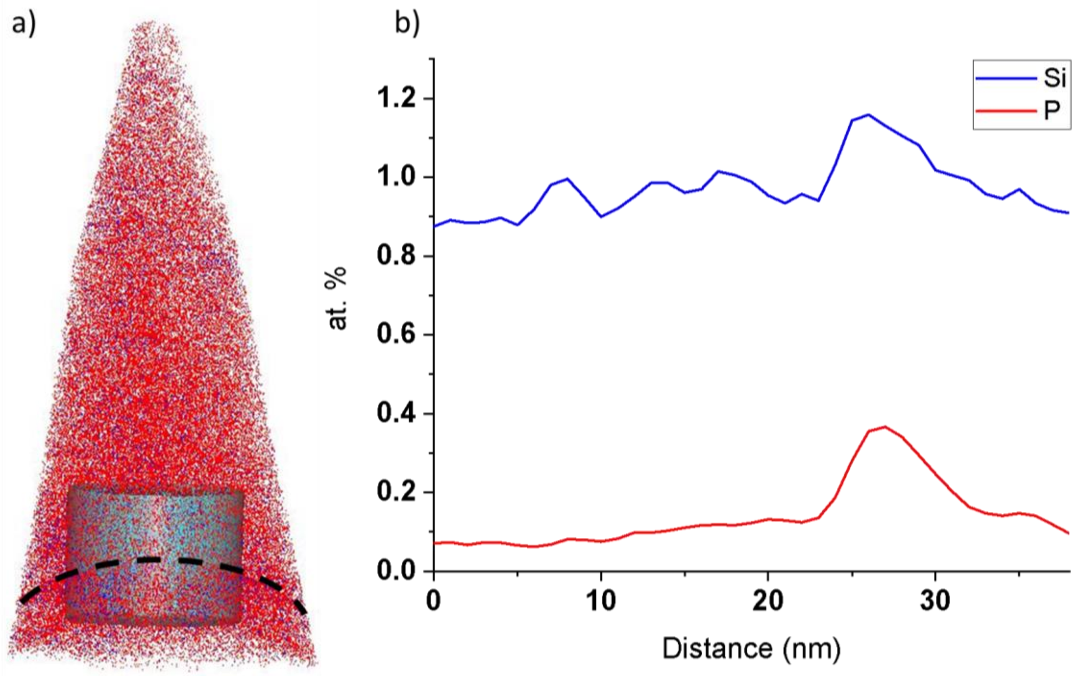

- **Significant segregation of Mn, Si, Ni, and P along grain boundaries**
- **Cu nanoprecipitates near/along grain boundaries, Ni-Mn-Si enriched precipitates along grain boundaries, needle like Cr precipitates**
- **Segregation behavior attributed to high point defect density/flux**

Concerns with thermal stability of nanostructured materials

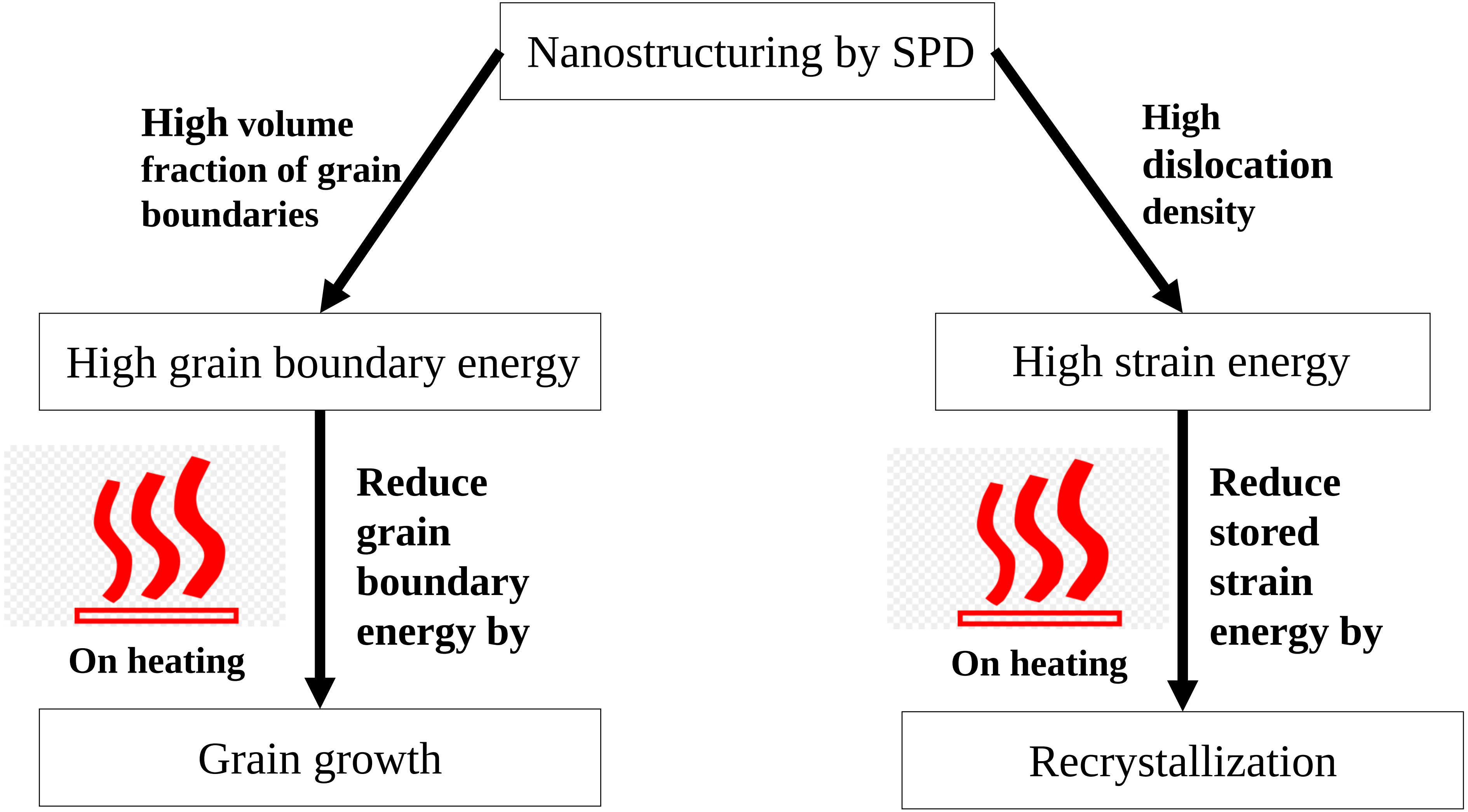

So, it is important to study the thermal stability of nanostructured materials.

Annealed microstructure of HPT G91

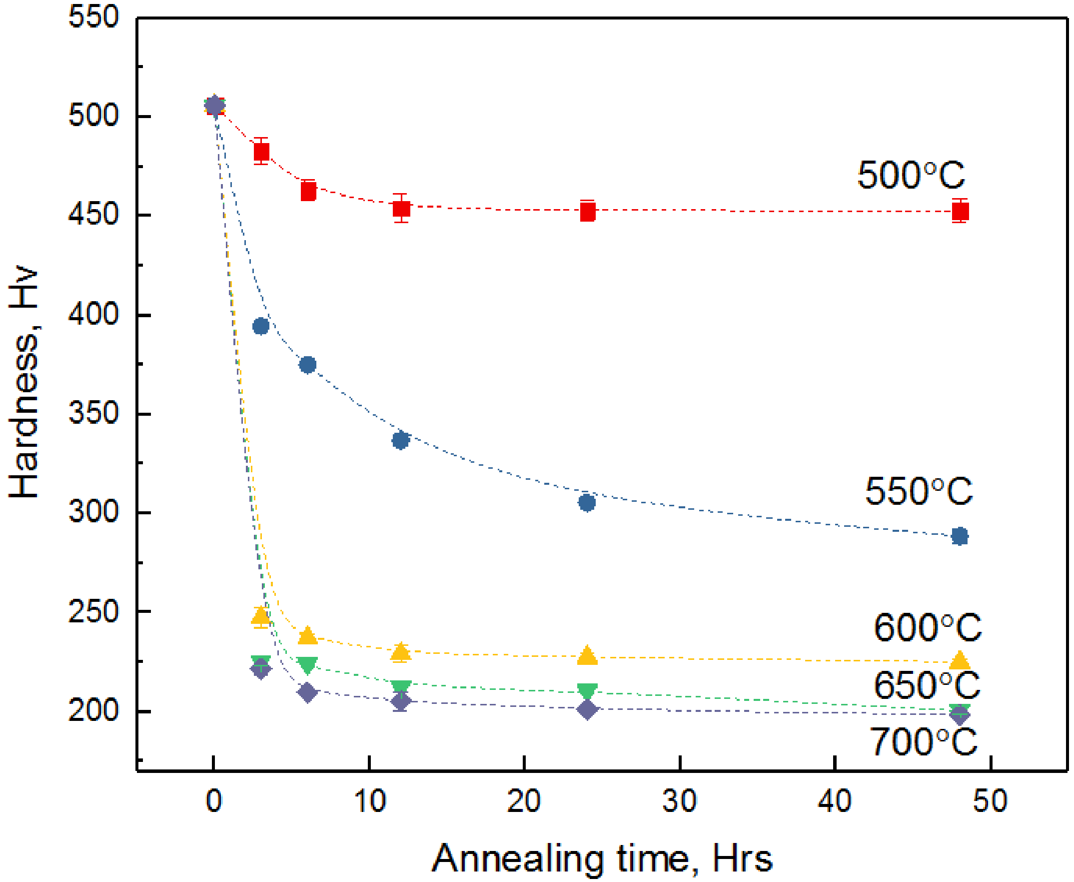

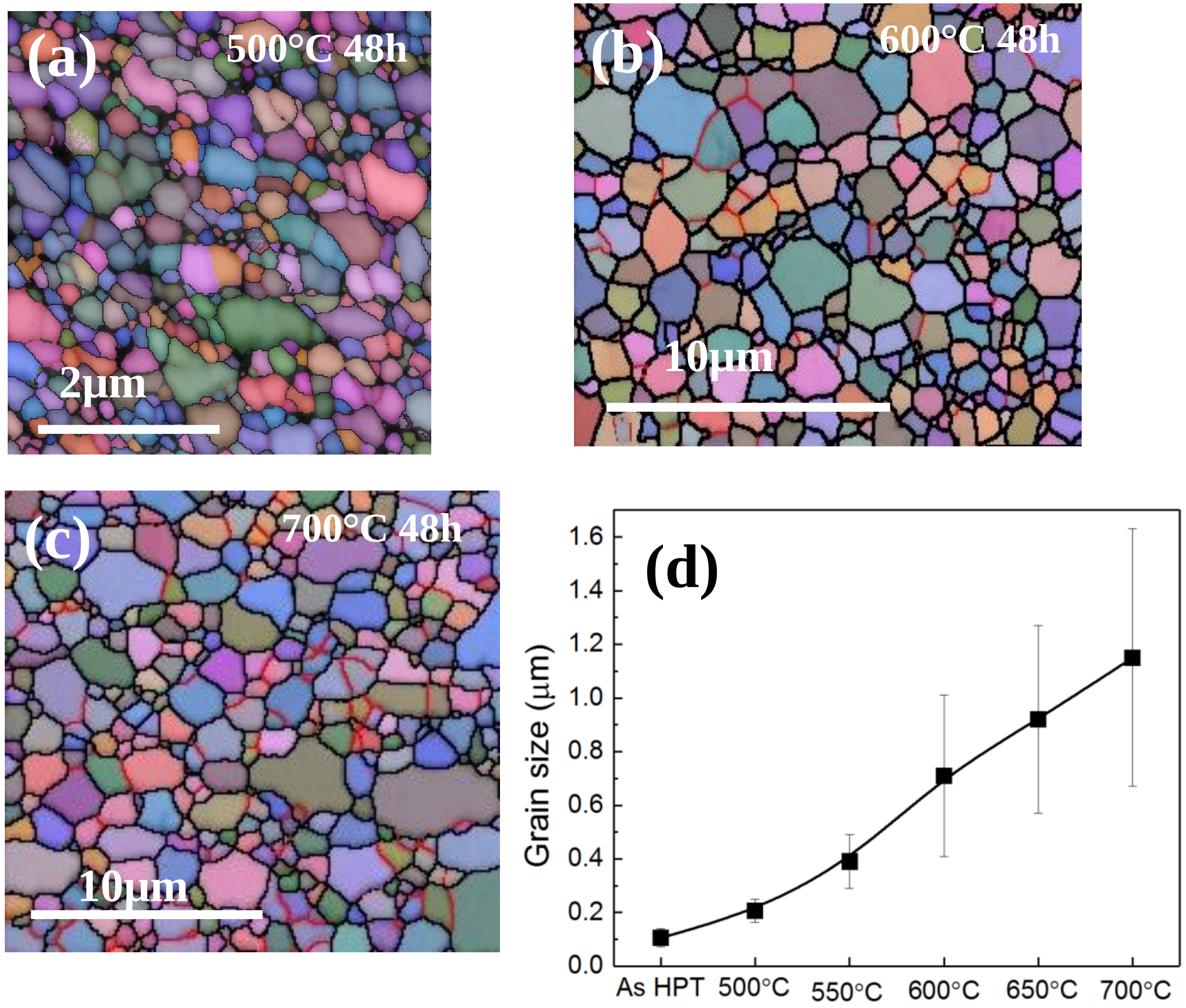

Grains grow in a homogenous manner (homogenous grain growth) at all annealing temperatures.

Grain growth leads to decrease in hardness

Annealed microstructure of ECAP G91

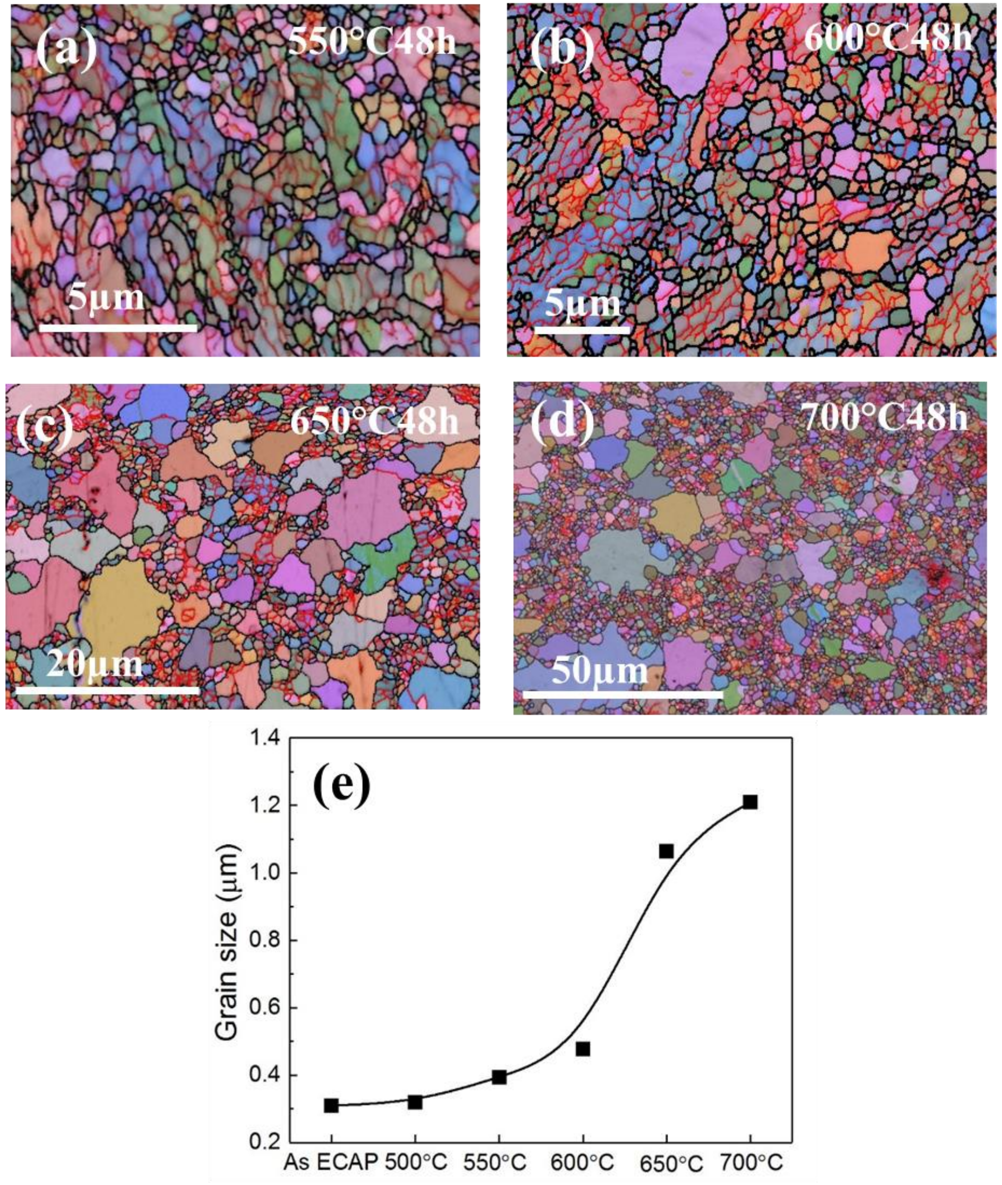

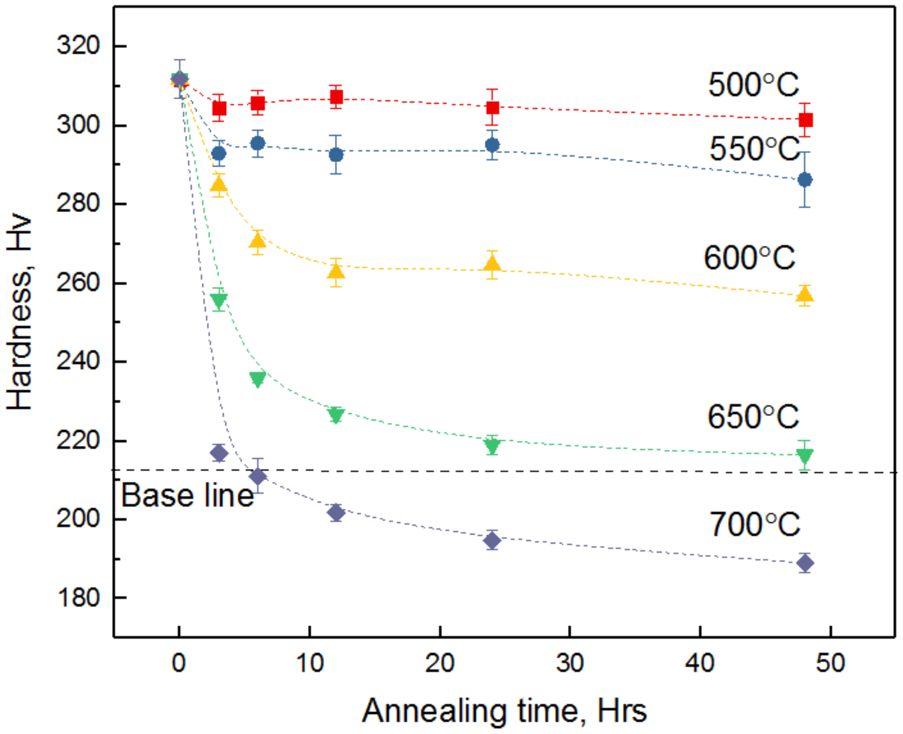

Microstructure is stable up to 500-550°C

Very inhomogeneous microstructure formed during annealing above 650°C, suggesting recrystallization.

Mechanism for Discontinuous Grain Growth in ECAP Grade 91

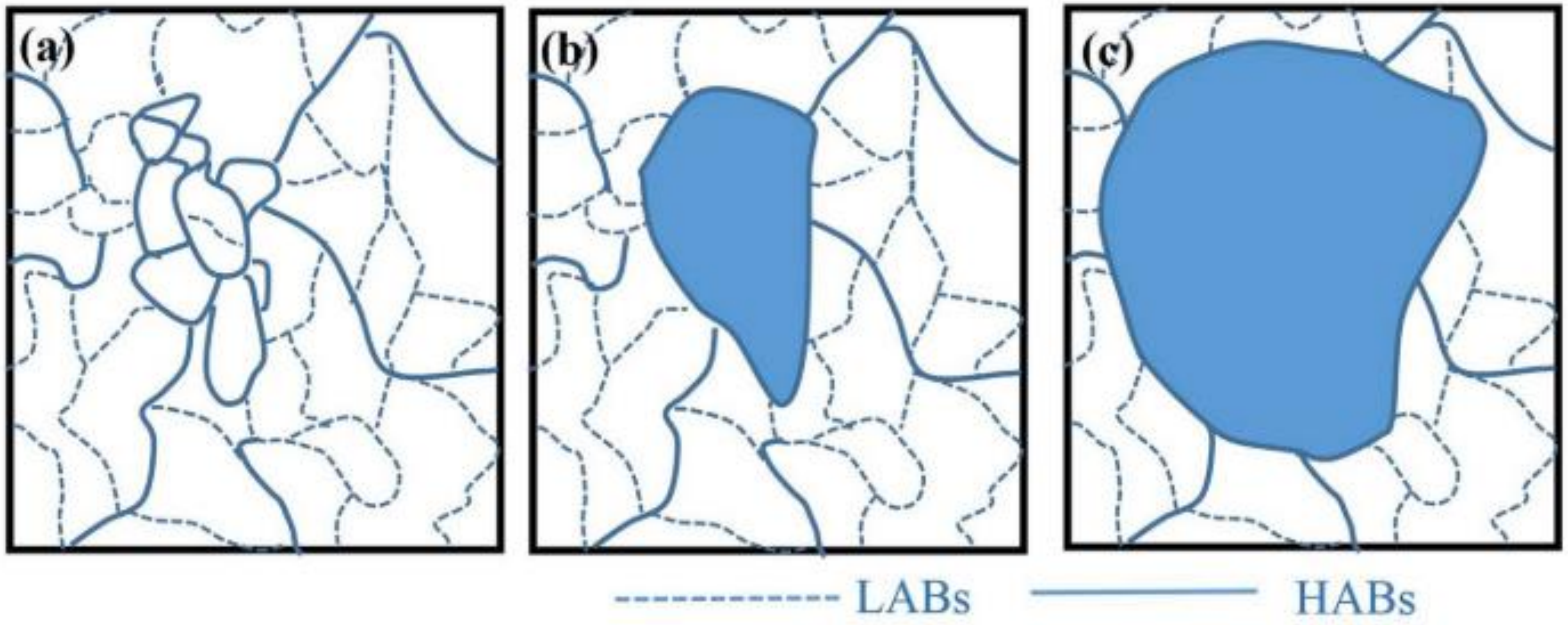

Fig. 11. Schematic diagram of discontinuous grain growth in the ECAP Fe-9Cr steel during annealing: (a-b) grain growth starts from the cluster of HABs, leading to a reduction in HABs; (c) the new grain consumes the thermally stable regions of LABs.

Annealed microstructure of ECAP Kanthal-D

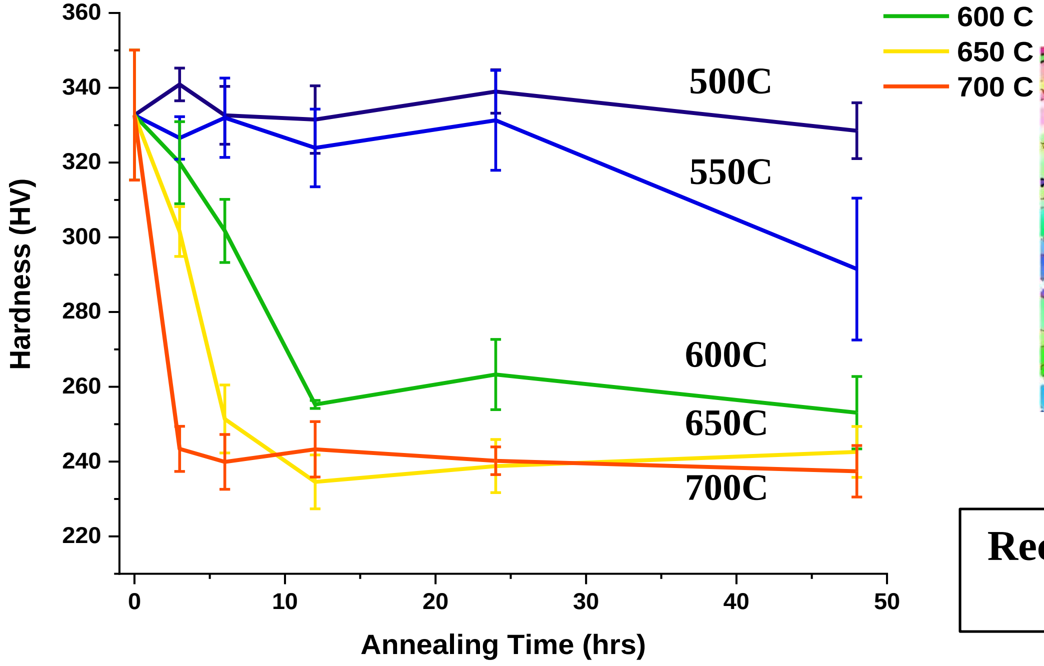

Onset of recrystallization

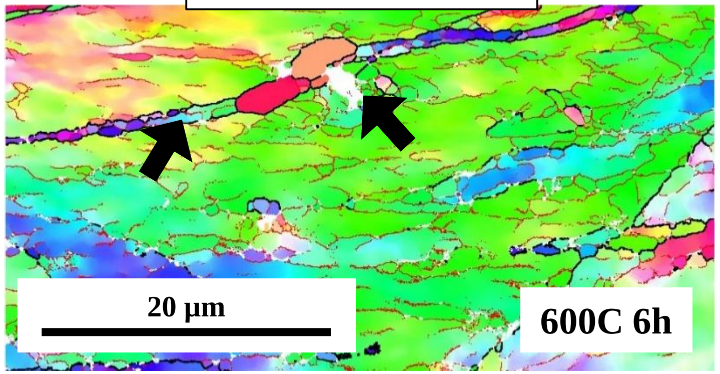

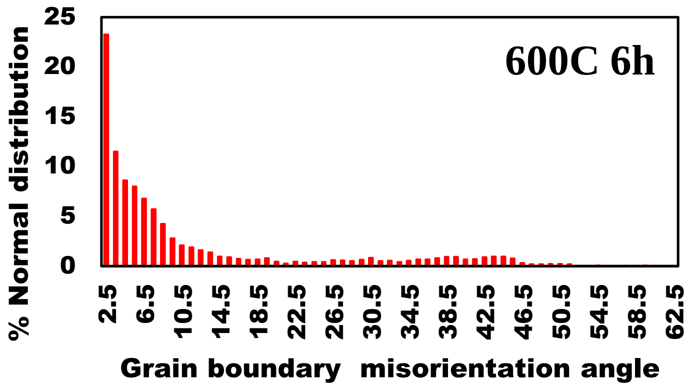

Recrystallization

Recrystallized grains

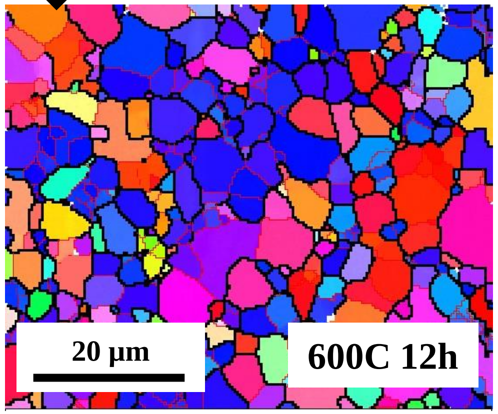

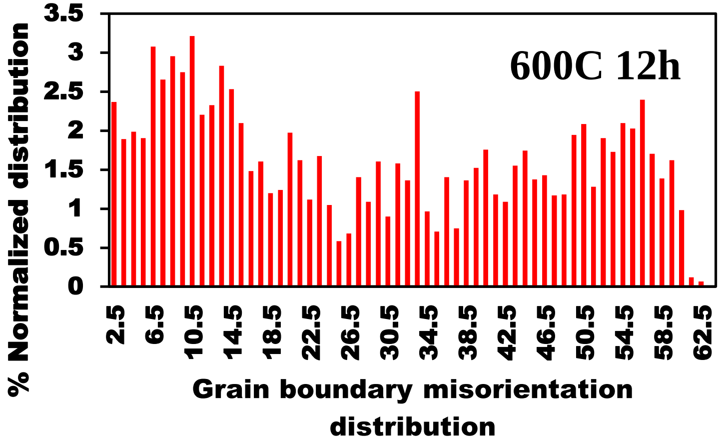

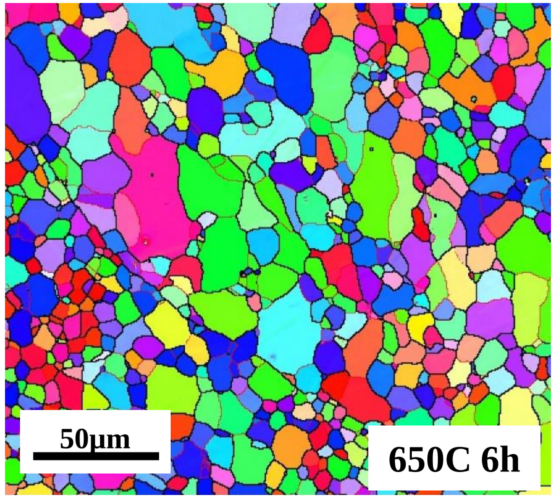

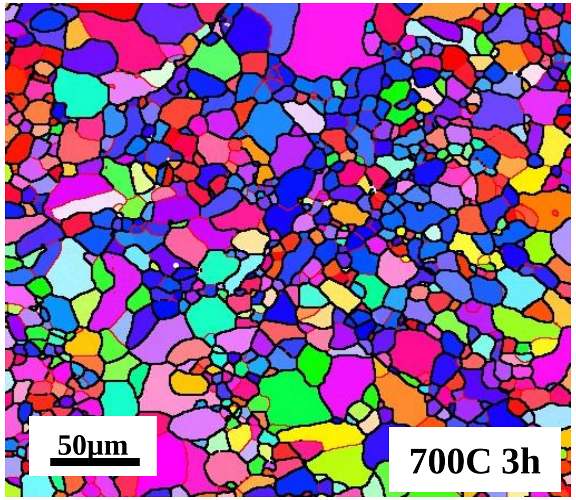

- Drastic drop in hardness also after annealing at 650 ^{o}C, 6h and 700 ^{o}C, 3h.
- This corresponds to recrystallization (evident from microstructure).
- Time to recrystallize comes down with increase in temperature.

Annealed microstructure of HPT Kanthal-D

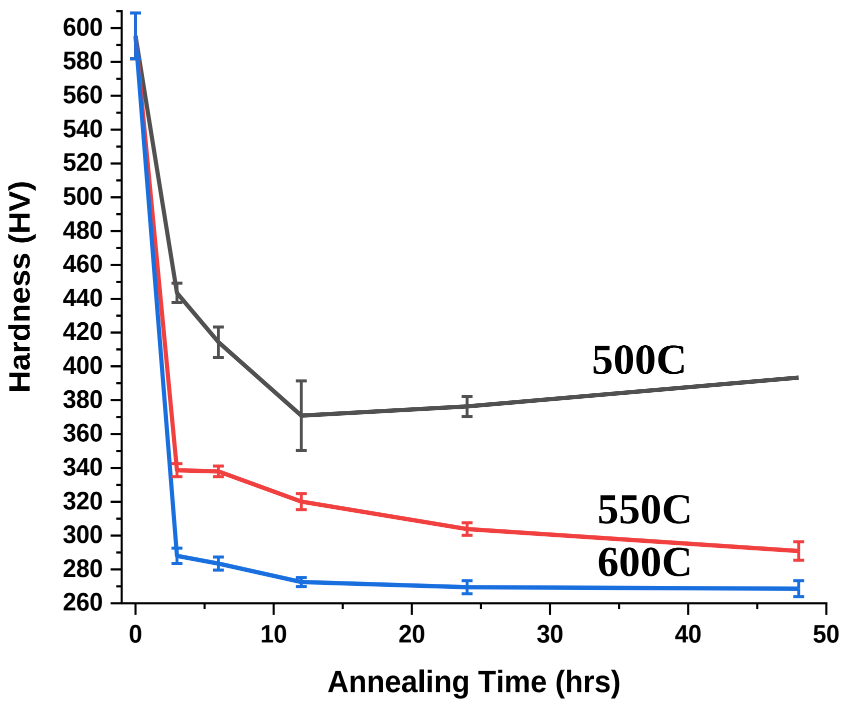

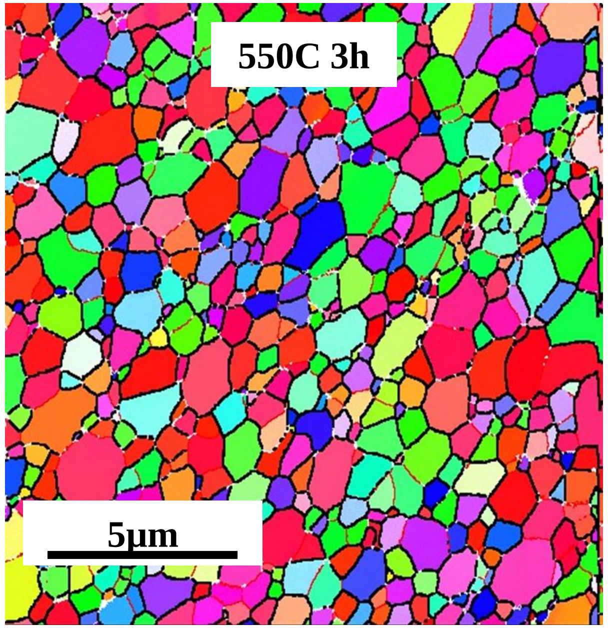

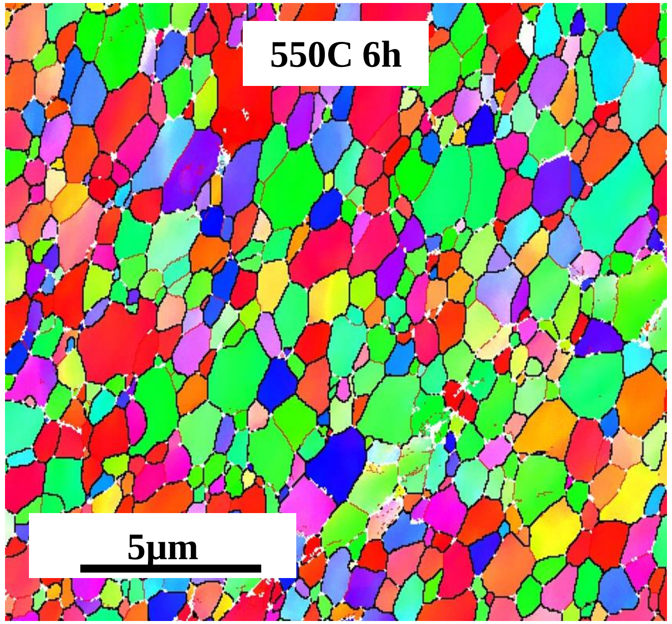

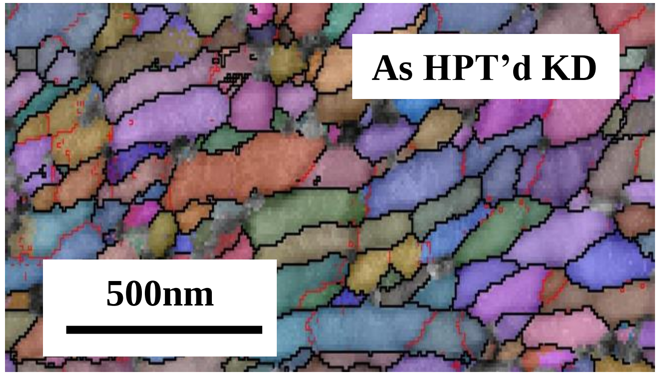

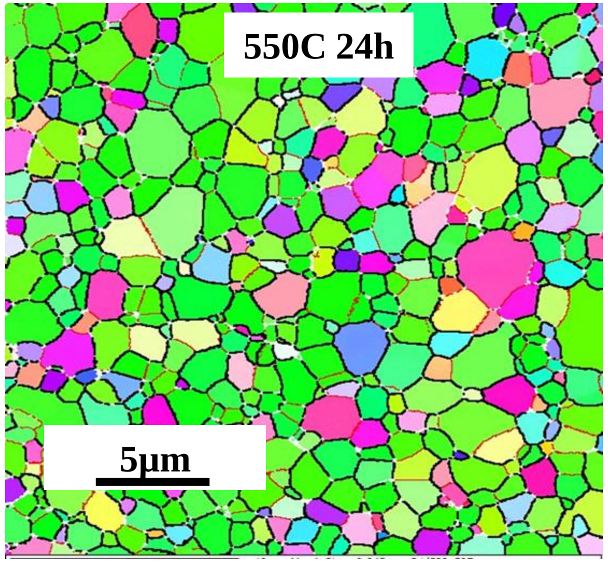

- HPT Kanthal-D thermally unstable at 500°C.
- Homogeneous grain growth due to stored grain boundary energy causing grain growth

Annealing Effects on ECAP 304

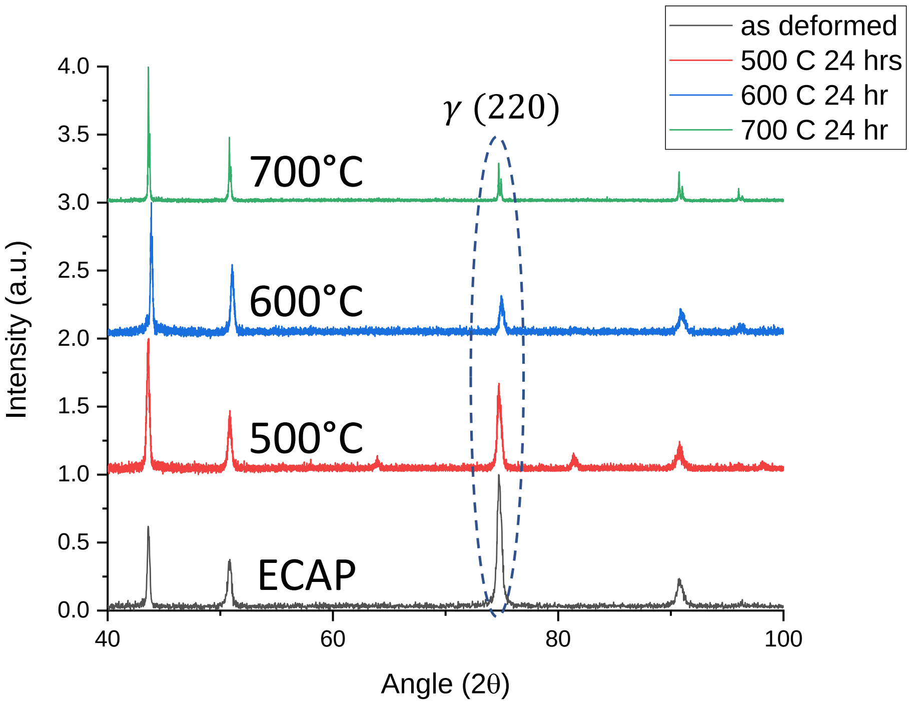

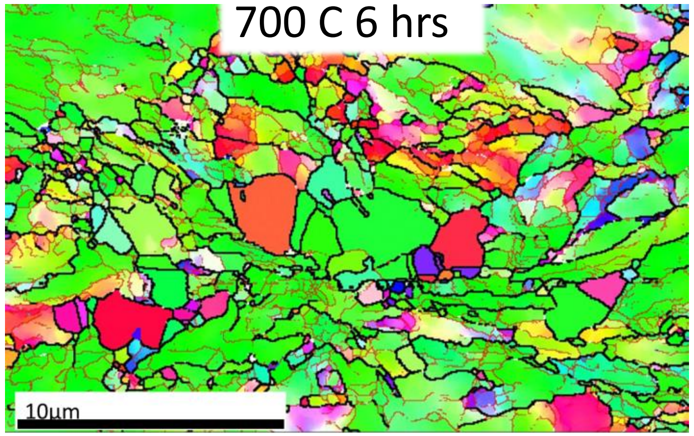

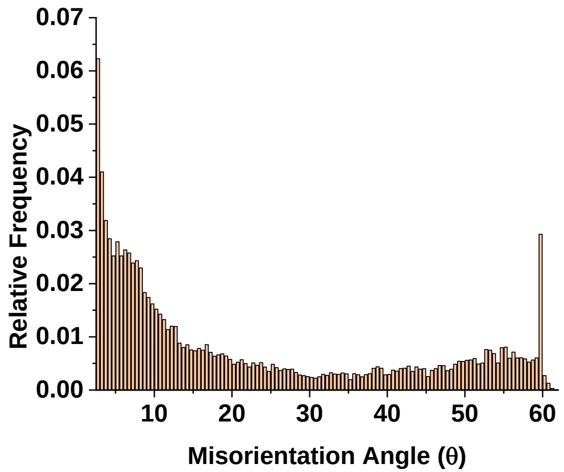

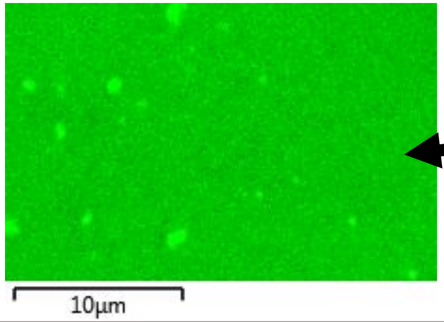

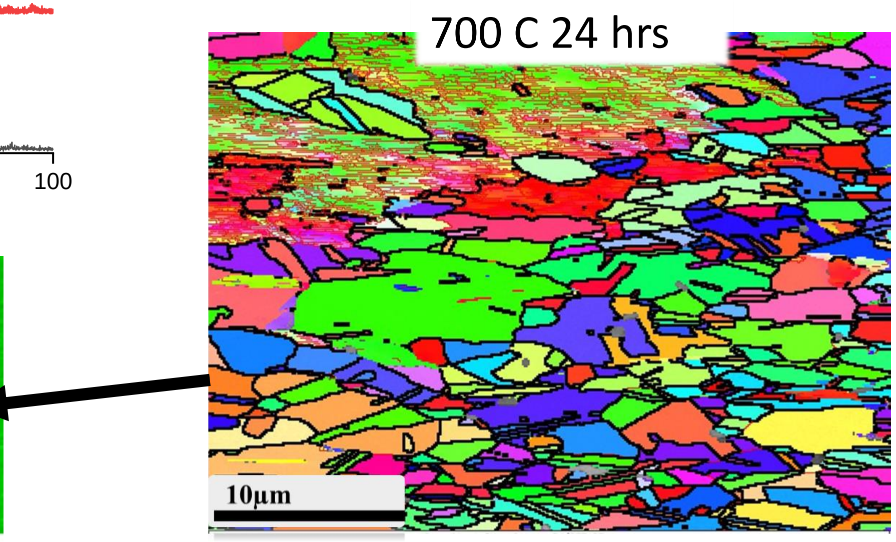

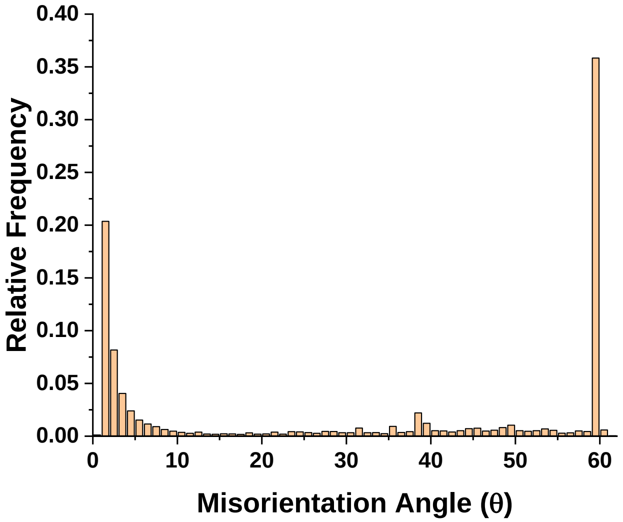

- No decrease in hardness after annealing below 700 C
- Increase in annealing temperature causes decrease in texture
- Significant recrystallization after annealing at 700 C, Cr enriched M_3C precipitation also occurs

Nanoindentation of Ion Irradiated 304

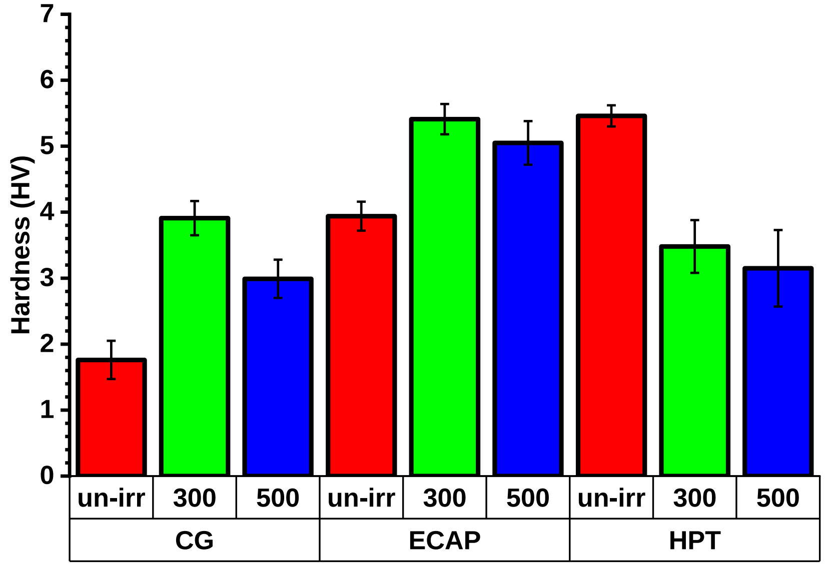

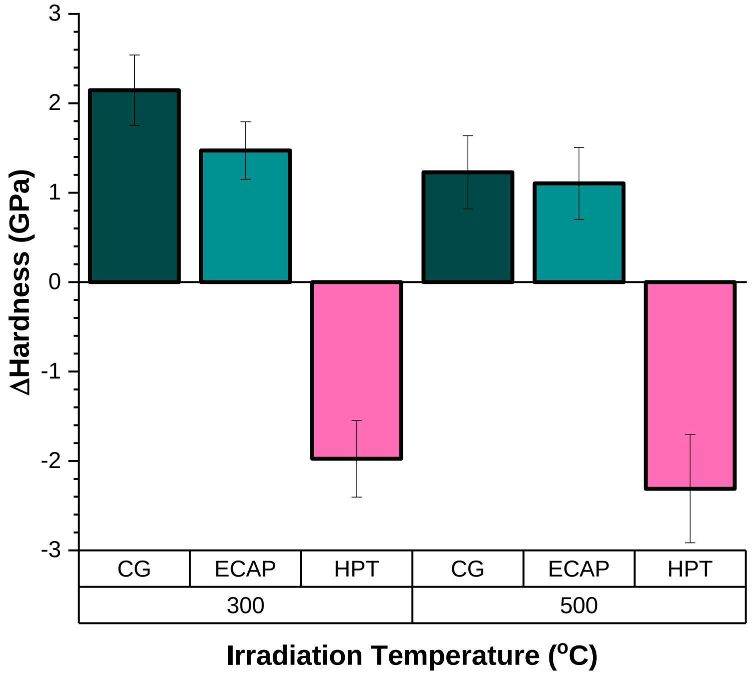

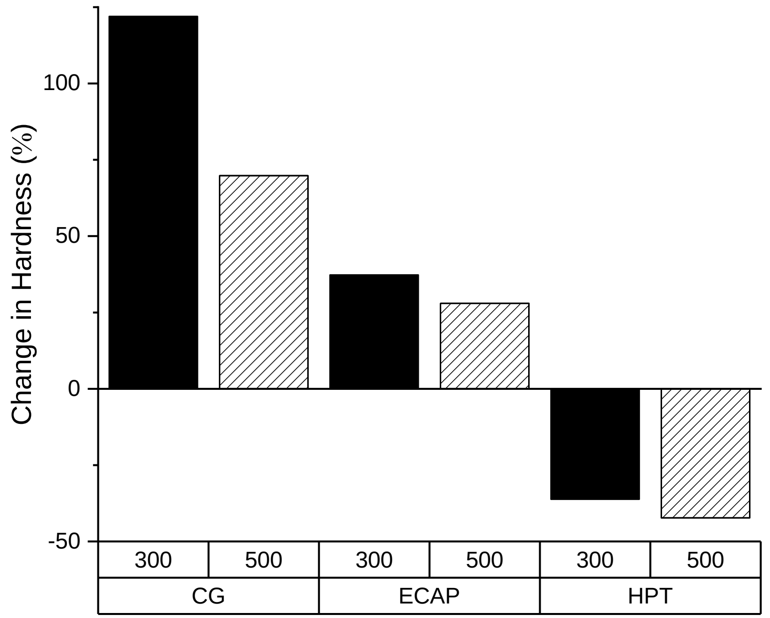

- **Nano-indentation performed to a depth of 150nm**
- **Although ECAP and CG have similar change in hardness at 500°C, the relative change in hardness is significantly reduced in ECAP sample**
- **Radiation induced softening of HPT 304 occurs due to radiation induced grain growth**

Effect of Grain Size on Ion Irradiation Induced Dislocation Loop Size

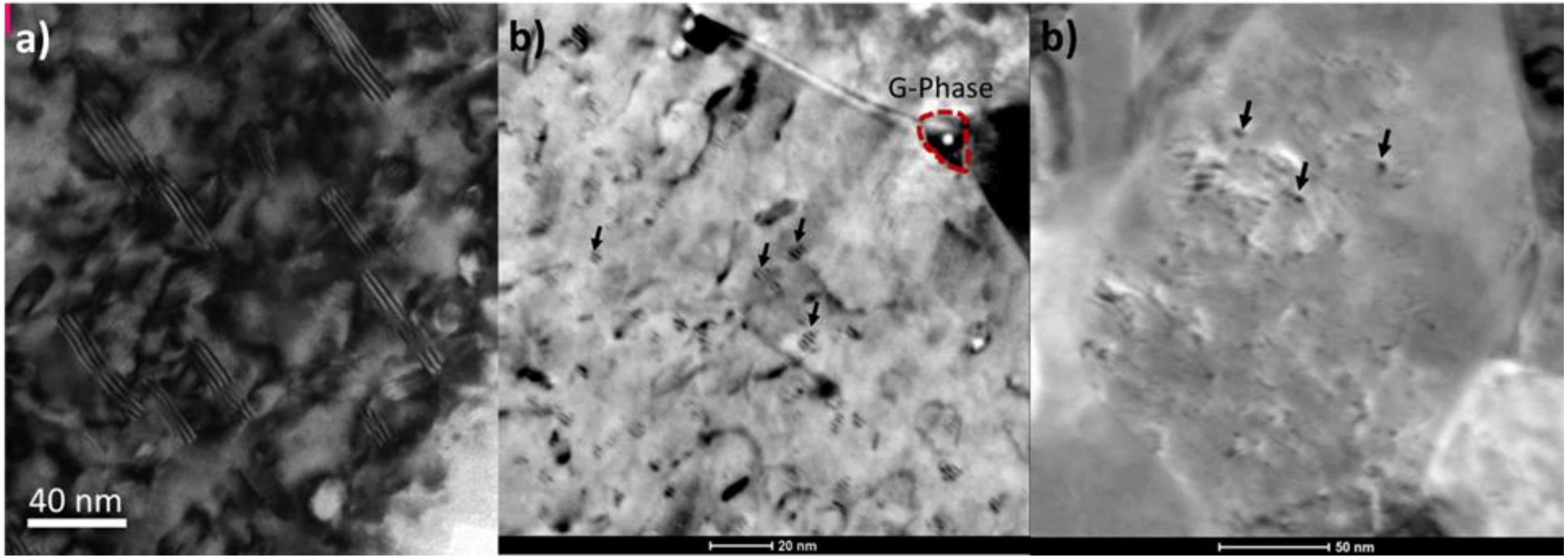

d_{loop}=33±10 nm

d_{loop}=6±3 nm

"black spot" defect clusters

- **Frank loop size decreases significantly with grain size**

Enhanced Austenite Stability of Nanostructured 304

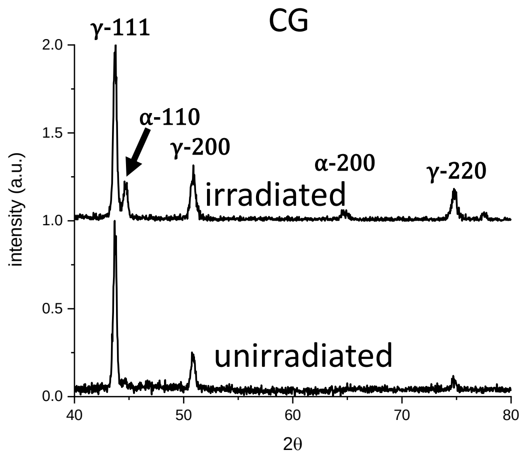

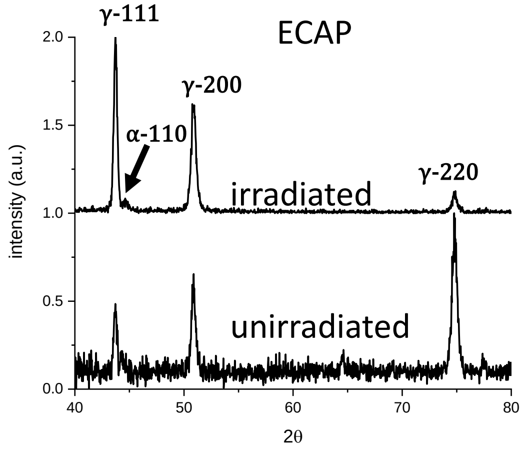

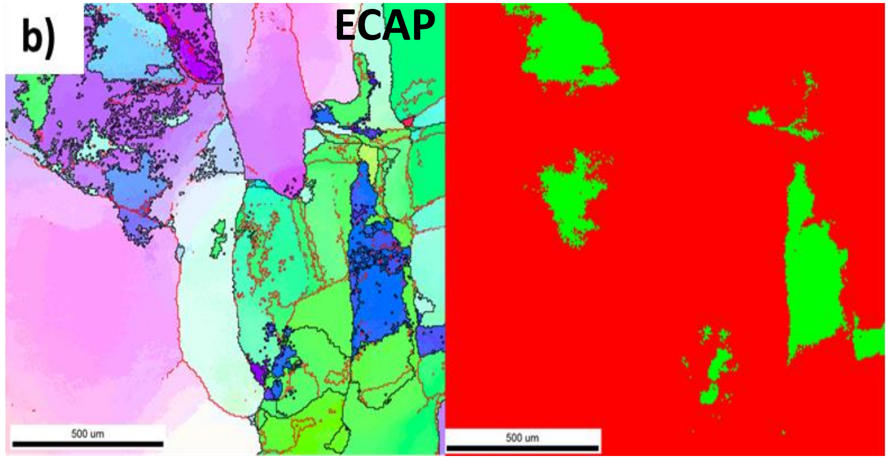

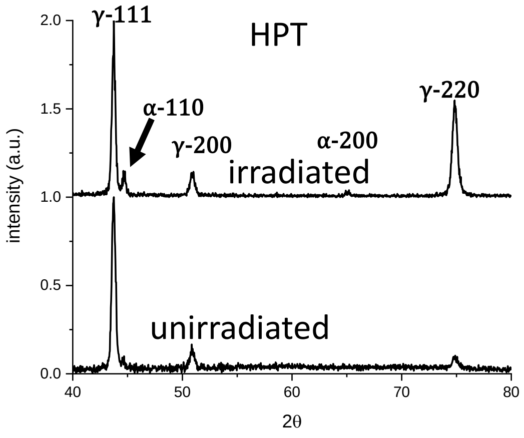

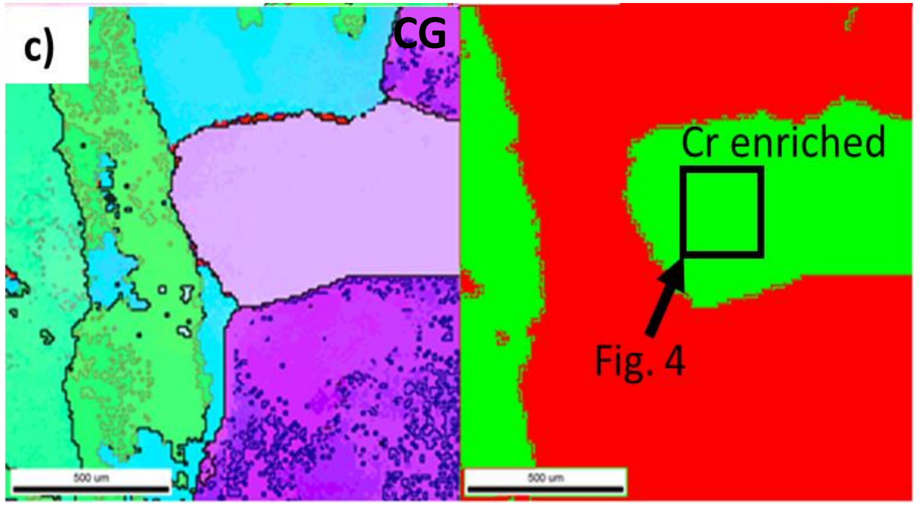

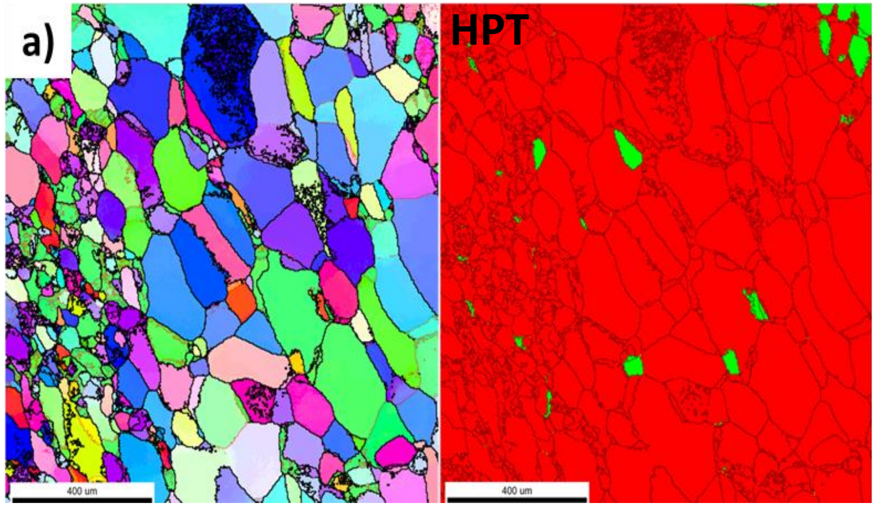

- **Nanostructured steels resistant to radiation induced austenite to ferrite transformation**

Enhanced Resistance to Radiation Induced Segregtion in HPT 304

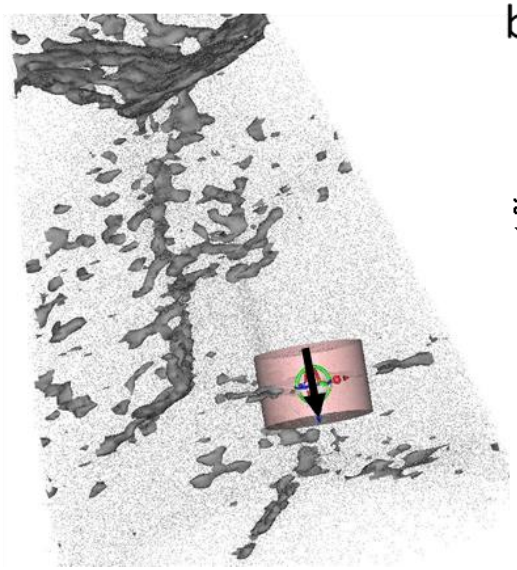

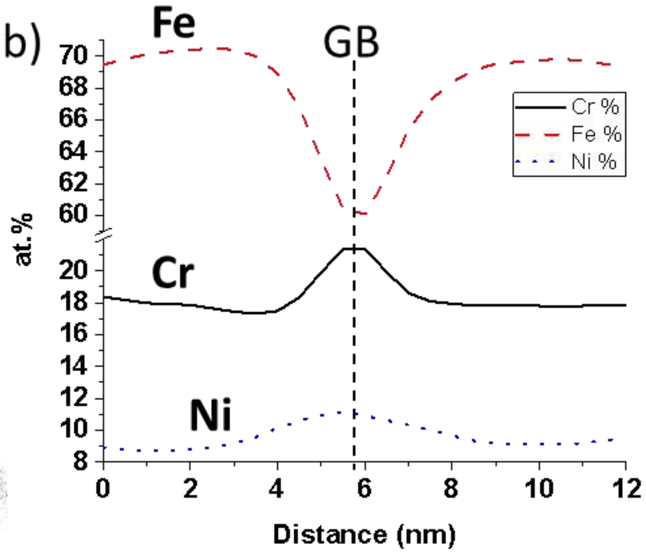

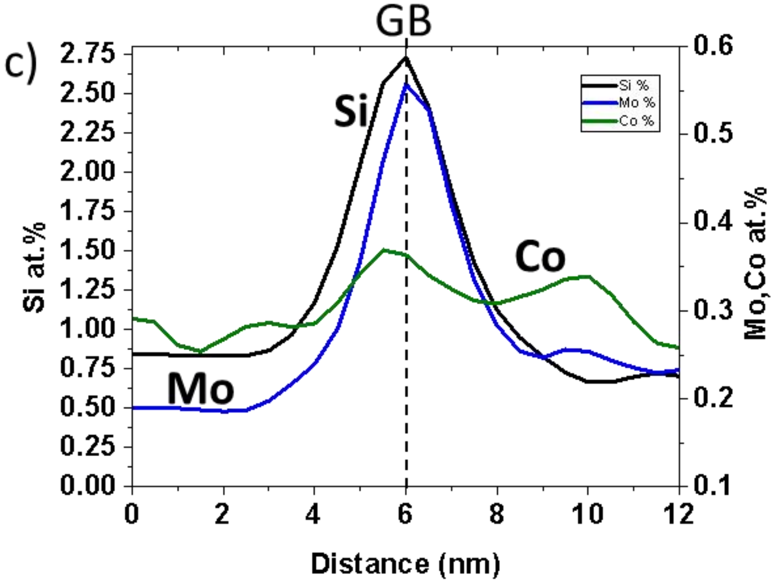

GB Description	# of GBs	Δat.% Fe	Δat.% Cr	Δat.% Ni	Δat.% Si	Δat.% Mo	Δat.% Co
Annealed	6	-3.5±2.4	+1.5±1.0	0	+0.6±0.4	1.2±0.7	0
Irradiated UFG	3	-11.6±6.0	-7.3±1.6	+13.8±3.0	+3.7±1.8	0	+0.2±0.1
Irradiated NC Grains	18	-4.3±1.4	-3.9±1.4	+5.3±1.8	+2.2±0.6	0	+0.1±0.04
Irradiated NC Cr enriched	4	-6.6±2.6	1.5±0.9	+2.0±1.0	+2.0±0.3	+0.4±0.1	0

Summary

- HPT and ECAP processing significantly improves the hardness/strength of steels.
- Grain size of HPT samples is smaller (<100nm) than ECAP samples (~500nm)
- ECAP samples have high number fraction of low angle grain boundaries, HPT samples contain mostly high angle grain boundaries
- SPD can cause segregation and precipitation
  - Cr carbides found in ECAP and HPT Kanthal-D
  - Ni and Si segregation towards grain boundaries in HPT 304 cause precipitation of G-Phase
  - Cu precipitation in HPT 304
- Large number fraction of low angle grain boundaries in ECAP samples enhance thermal stability
  - Primary coarsening mechanism is recrystallization in ECAP samples vs grain growth in HPT samples
- Ion irradiation of 304 shows enhanced radiation tolerance of nanostructured austenitic steels
  - Resistance to radiation induced hardening, smaller loops sizes, enhanced austenite stability, and reduced segregation

List of Publications

- A. Ganeev, M. Nikitina, V. Sitdikov, R. Islamgaliev, A. Hoffman, H. Wen, Effects of the tempering and high-pressure torsion temperatures onmicrostructure of ferritic/martensitic steel grade 91, Materials (Basel). 11 (2018). doi:10.3390/ma11040627.
- A. Hoffman, H. Wen, R. Islamgaliev, R. Valiev, High-pressure torsion assisted segregation and precipitation in a Fe-18Cr-8Ni austenitic stainless steel, Mater. Lett. 243 (2019) 116–119. doi:10.1016/j.matlet.2019.02.030.
- J. Duan, H. Wen, C. Zhou, R. Islamgaliev, X. Li, Evolution of microstructure and texture during annealing in a high-pressure torsion processed Fe-9Cr alloy, Materialia. 6 (2019) 1–5. doi:10.1016/j.mtla.2019.100349.
- J. Duan, H. Wen, C. Zhou, X. He, R. Islamgaliev, R. Valiev, Discontinuous grain growth in an equal-channel angular pressing processed Fe-9Cr steel with a heterogeneous microstructure, Mater. Charact. (2019) 110004. doi:10.1016/J.MATCHAR.2019.110004.
- M. Arivu, A. Hoffman, J. Duan, H. Wen, R. Islamgaliev, R. Valiev, Severe plastic deformation assisted carbide precipitation in Fe-21Cr-5Al alloy, Mater. Lett. 253 (2019) 78–81. doi:10.1016/j.matlet.2019.05.139.

List of Publications in Progress

- M. Arivu, A. Hoffman, J. Duan, H. Wen, R. Islamgaliev, R. Valiev, “Comparison of Thermal stability of Equal Channel Angular Pressed and High Pressure Torsioned Fe-21Cr-5Al alloy”, to be submitted to MSEA.
- J. Duan, H. Wen, C. Zhou, X. He, R. Islamgaliev, R. Valiev, Annealing behavior of high-pressure torsion processed Fe-9Cr steel, Mater Charact, (under review).
- J. Duan, H. Wen, L. He, K. Sridharan, R. Islamgaliev, R. Valiev, “Improving the irradiation resistance in Fe-9Cr steel through grain refinement” (in preparation).
- A. Hoffman, M. Arivu, H. Wen, L. He, K. Sridharan, X. Wang, W. Wrong, X. Liu, L. He, Y. Wu, "Enhancing Resistance to Irradiation Induced Ferritic Transformation Through Nano-structuring of Austenitic Steels", to be submitted to Acta Materialia
- A. Hoffman, M. Arivu, I. Robin, H. Wen, R. Valiev, R. Islamgaliev, H. Pommerenke, N. Curtis, V. DeLibera, M. Gougar, "Enhanced Austenite Stability of Ultra-fine Grained Austenitic Steel" To be submitted to MSEA
- M. Arivu, A. Hoffman, H. Wen, L. He, K. Sridharan, J. Burns, "Effect of Grain Size on Ion Irradiated 304 Austenitic Steel" To be submitted to Journal of Nuclear Materials
- A. Hoffman, Y. Zhang, M. Arivu, H. Wen, "Competing Effects of Kinetic and Thermodynamic Segregation in Ion Irradiated Nanocrystalline Austenitic Steel", to be submitted to Scripta Materialia

Neutron irradiation

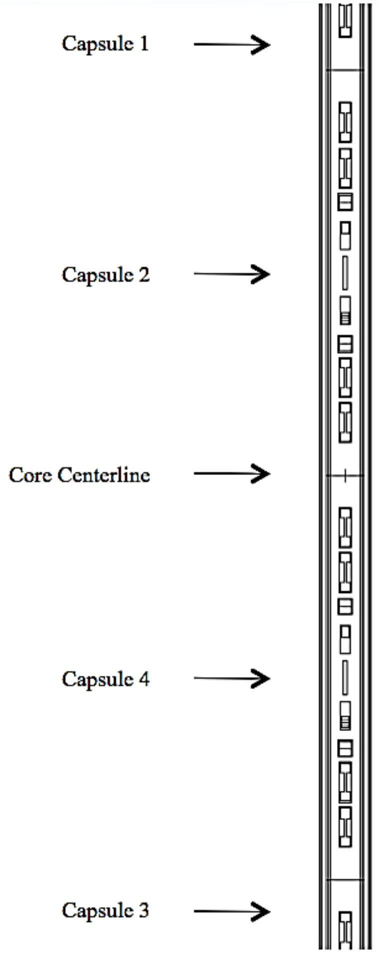

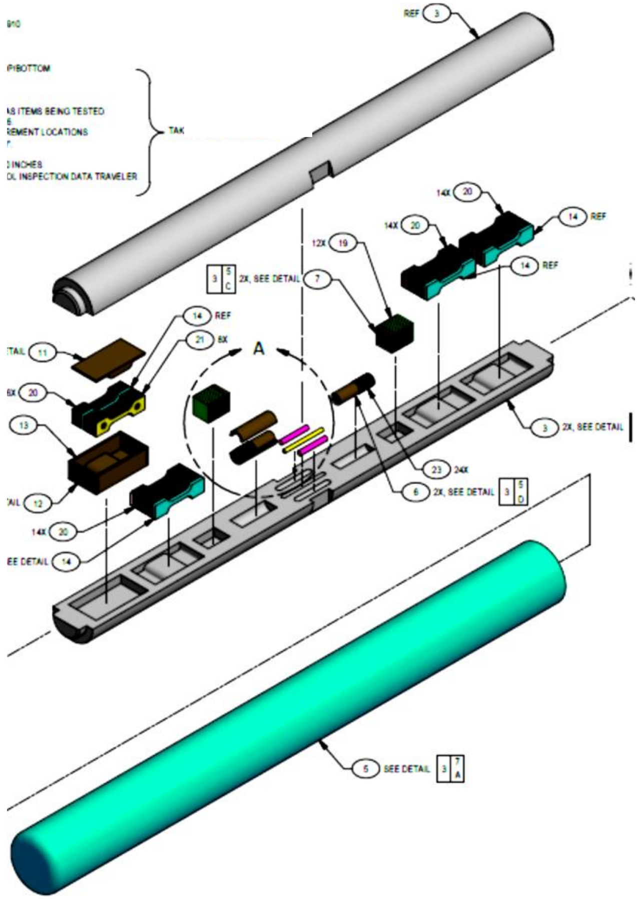

- Conducted at Advanced Test Reactor
  (Samples in ATR since June 2018)
- Four irradiation conditions and capsules
  - Capsule 1 at 300 ºC to 2 DPA (8 months)
  - Capsule 2 at 300 ºC to 6 DPA (2 years)
  - Capsule 3 at 500 ºC to 2 DPA (8 months)
  - Capsule 4 at 500 ºC to 6 DPA (2 years)
- Tensile, hardness and TEM specimens
- Non-instrumented standard capsule experiments
- Melt wires and SiC to monitor temperature
- Flux wires to measure flux
- ~500 specimens in total

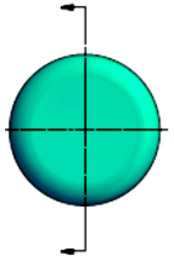

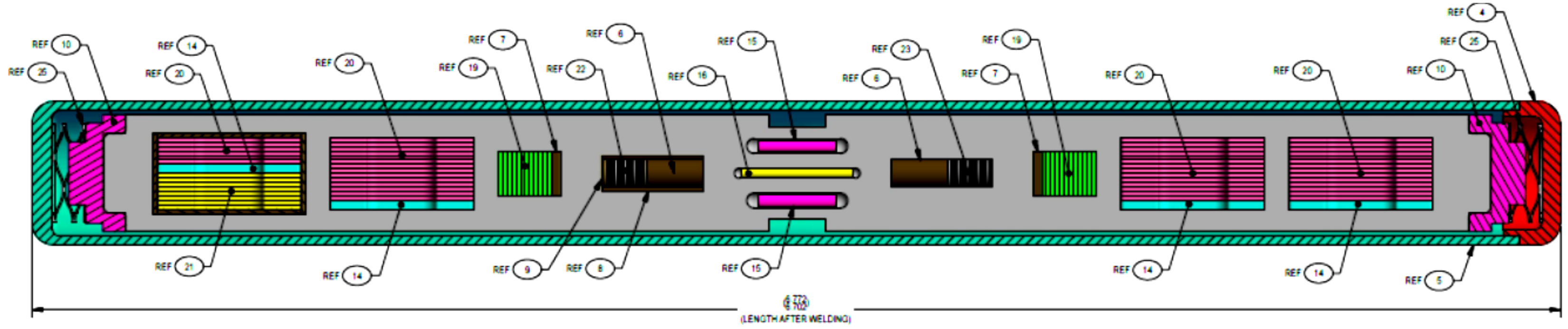

AMM Program Review

Dec 17–18

Enhancing irradiation tolerance of steels via nanostructuring by innovative manufacturing techniques

MISSOURI S&T

Haiming Wen
wenha@mst.edu

Department of Materials Science and Engineering
Department of Mining and Nuclear Engineering
Missouri University of Science and Technology

Questions?

Microstructure of As-HPTed Kanthal-D

Transmission Kikuchi Diffraction

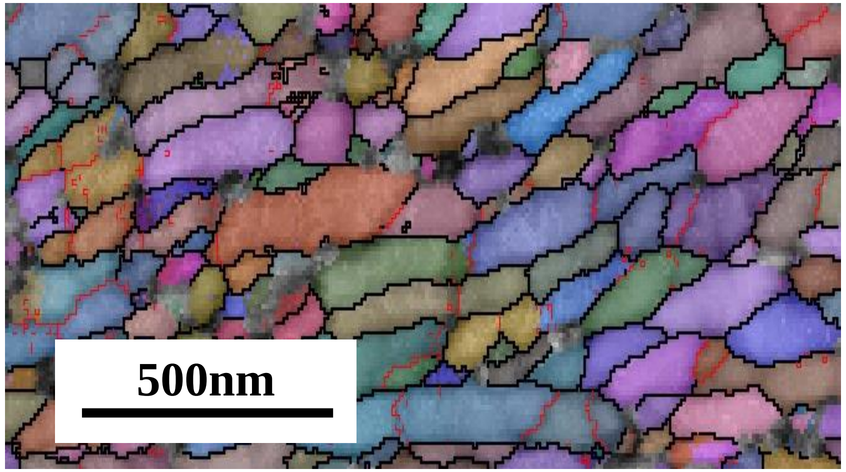

Longitudinal direction

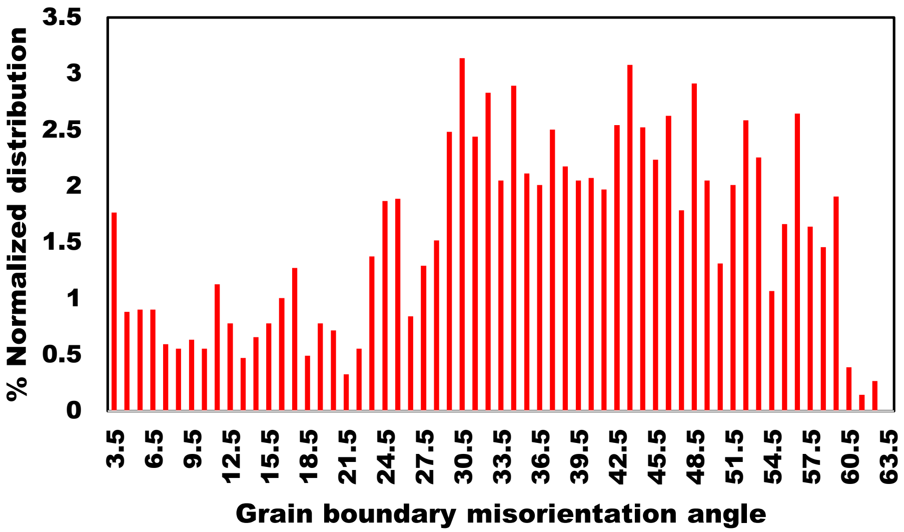

Transmission Electron Microscopy

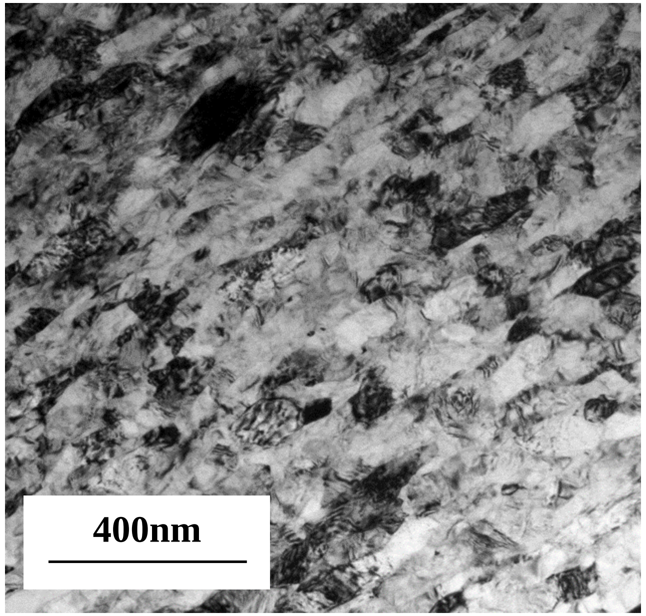

- Average grain size of 75 ± 40nm with an equiaxed microstructure.
- The volume fraction of high angle grain boundaries is 80%.
- 20% higher than ECAP KD (higher grain boundary energy).